

Received August 30, 2020, accepted October 16, 2020, date of publication October 21, 2020, date of current version November 6, 2020.

Digital Object Identifier 10.1109/ACCESS.2020.3032748

# A Novel Low-Complexity Estimation of Sampling and Carrier Frequency Offsets in OFDM Communications

ARIK ROTEM<sup>ID</sup>, (Student Member, IEEE), AND RON DABORA<sup>ID</sup>, (Senior Member, IEEE)

Department of Electrical and Computer Engineering, Ben-Gurion University, Be'er-Sheva 8410501, Israel

Corresponding author: Ron Dabora (ron@ee.bgu.ac.il)

This work was supported by the Israel Science Foundation under Grant 1685/16.

**ABSTRACT** This paper presents a novel low-complexity sequential, blind, pilot-assisted estimator for the sampling frequency offset (SFO) and the carrier frequency offset (CFO), for orthogonal frequency-division multiplexing (OFDM) communications. The proposed algorithm processes the received subcarriers to obtain a cost function which depends only on a single unknown parameter at a time, either the SFO or the CFO, as well as on a specifically designed auxiliary parameter, while ignoring the noise. Then, by computing the cost function at a few selected values of the auxiliary parameter, an explicit estimator for each unknown parameter is derived, thereby avoiding the need for a search. To the best of our knowledge, this is the first time such a deterministic approach is applied to the joint estimation of the SFO and the CFO. Moreover, the proposed estimator does not require knowledge of the channel coefficients at the pilot subcarriers, and achieves good performance with a relatively small number of pilot symbols, which results in a low computational complexity. Simulation results show that at low computational complexity, there are many scenarios in which the new estimator achieves smaller estimation errors compared to other existing methods.

**INDEX TERMS** OFDM, synchronization, carrier frequency offset, sampling frequency offset.

## I. INTRODUCTION

Orthogonal frequency-division multiplexing (OFDM) is a multicarrier modulation scheme which is widely used in current wireless and wireline communications standards, and is also a major candidate for future communications networks [1], [2]. In practical OFDM communications systems, offsets between the frequencies of the RF oscillators and of the sampling clocks at the transmitter and at the receiver, referred to as carrier frequency offset (CFO) and sampling frequency offset (SFO), respectively, result in a loss of orthogonality between the subcarriers of the received OFDM symbols, which induces a loss in communications performance. It follows that facilitating high rate, reliable OFDM communications requires a fast and accurate SFO and CFO estimation [3].

The sensitivity of OFDM performance to SFO and to CFO has motivated a very large body of works on SFO and CFO estimation. In the following we focus only on

The associate editor coordinating the review of this manuscript and approving it for publication was Derek Abbott<sup>ID</sup>.

a few of the most closely related works: The work in [4] proposed a pilot-aided blind suboptimal maximum likelihood (ML)-oriented algorithm for estimating the CFO and the SFO in OFDM systems, using a one-dimensional grid search, which leads to an algorithm of a practical complexity. In [5], data-aided estimation of the CFO and the SFO was realized based on the Taylor expansion of the ML cost function, which replaced the grid search with the task of finding the roots of a polynomial. The work in [6] derived an efficient blind CFO estimator using three values of a cost function, obtained by oversampling a single OFDM symbol and then applying a time-shift followed by downsampling, leading to two separate OFDM symbols used for generating the cost function. In [7] a low complexity CFO estimator is derived by summing the products of the magnitudes of received subcarriers over two consecutive OFDM symbols. Each subcarrier used by the estimator is constrained to using constant modulus signaling. The estimate is then obtained by computing a cost function at three distinct values. In [8], a joint estimator of the SFO and the sampling phase offset is derived by using an approximate log-likelihood function derived by imposing

Gaussianity on the received signal component. Then, a least-squares estimator is derived by further approximating the log-likelihood function. In [9] SFO and CFO estimation is derived by using non-uniformly distributed continual pilots. As non-uniformity of the pilot distribution introduces bias into the resulting least-squares estimators, the authors suggest to partition the pilots into two subsets such that the bias is eliminated. Lastly, the work in [10] proposed a blind CFO and SFO estimator based on taking two fast Fourier transform (FFT) windows within the same OFDM symbol, a synchronized window and a shifted window, from which the conditional distribution of the shifted version given the synchronized version is derived. Then, an estimator for the SFO based on a single dimensional grid search is obtained and a further simplified solution is proposed. Subsequently, the CFO is estimated as a deterministic function of the estimated SFO. In the current paper we utilize the approach proposed in [6] for CFO estimation, to derive a very low complexity blind estimator for the SFO and the CFO. The estimator uses a small number of pilot symbols for estimating first the SFO. Then, the estimated SFO is used for eliminating its impact on the received signal in order to facilitate CFO estimation via a subsequent low complexity function.

### A. MAIN CONTRIBUTIONS

In this work we derive a blind, pilot-assisted, sequential SFO and CFO estimation scheme. As the optimal joint SFO and CFO estimation scheme has a high computational complexity, see e.g., [4], our focus in this work is on deriving an estimation algorithm whose performance is superior to that of the state-of-the-art, while maintaining a low computational complexity, as compared to the state-of-the-art. The proposed estimation scheme applies a specifically designed processing to the received signal, while ignoring the additive noise, and assuming the channel remains approximately the same over two subsequent symbols. The first processing eliminates the dependence of the processed samples on the CFO and leads to an *explicit* SFO estimator. Subsequently, the estimated SFO is used by a second processing to obtain two *explicit* estimators for the CFO. By obtaining explicit expressions the complexity associated with a search is avoided. The processing applies specifically designed phase shifts to the processed samples, modifying and extending the idea employed in [6] for CFO estimation, in which the cost function was obtained from a single OFDM symbol, by summing over all frequency domain values of a function of the oversampled received symbol and a test signal. The idea of [6] is extended and adapted to *joint SFO and CFO estimation using only specific subcarriers over two subsequent symbols*. Thus, our cost functions are completely different from those used in previous joint SFO/CFO estimation works, e.g., in [9], as is evident from the numerical evaluations: There are many channels in which our newly proposed estimator is superior to the baseline scheme of [9] and there are channels in which the baseline scheme is superior to our proposed estimator. It follows that the main novelty lies in the proposed processing which facilitates a

simple extraction of the SFO and the CFO, while maintaining an overall low computational complexity.

The rest of this paper is organized as follows: Section II presents the model of the received OFDM signal. Section III derives the new low-complexity estimator for the SFO as well as two new low-complexity estimators for the CFO. Section IV reviews in detail the baseline schemes, suggests an improvement to one of these schemes, and presents a detailed analysis of the computational complexity for the proposed estimators as well as for the existing methods. Simulation results and numerical performance are presented in Section V together with a discussion. Lastly, conclusions are highlighted in Section VI.

### B. NOTATIONS

We denote the convolution operator with ‘ $\star$ ’, and use  $\delta[n]$  to denote the *Kronecker* impulse function. Stochastic expectation and complex conjugate are denoted with  $\mathbb{E}\{\cdot\}$  and  $(\cdot)^*$ , respectively. The sets of integers and of real numbers are denoted by  $\mathcal{Z}$  and  $\mathcal{R}$ , respectively. For an arbitrary set  $\mathcal{A}$ , we use  $|\mathcal{A}|$  to denote its cardinality.

## II. MODEL OF THE RECEIVED OFDM SIGNAL

Let  $N_{sc}$  denote the number of subcarriers in an OFDM symbol and  $D_{m,k}$  denote the complex random data symbol modulating the  $k$ -th subcarrier of the  $m$ -th OFDM symbol,  $k \in [0, N_{sc} - 1]$ ,  $m \in \mathcal{Z}$ . We assume that the data symbol  $D_{m,k}$  is selected uniformly from a finite, zero mean and proper complex set of constellation points  $\mathcal{D}$ , in an independent and identically distributed (i.i.d) manner over  $k$  and  $m$ . Thus,

$$\mathbb{E}\{D_{m,k}D_{\tilde{m},\tilde{k}}^*\} = \sigma_D^2 \cdot \delta[m - \tilde{m}] \cdot \delta[k - \tilde{k}] \quad (1a)$$

$$\mathbb{E}\{D_{m,k}\} = 0, \quad \mathbb{E}\{D_{m,k}D_{\tilde{m},\tilde{k}}\} = 0 \quad (1b)$$

The  $m$ -th OFDM symbol is generated from  $\{D_{m,k}\}_{k=0}^{N_{sc}-1}$  by applying an inverse discrete Fourier transform (IDFT) of size  $N_{sc}$  and then adding a cyclic prefix (CP) of length  $N_{cp}$  samples at the beginning of the IDFT output sequence. It follows that the length of the resulting OFDM symbol in time samples is  $N_{sym} = N_{sc} + N_{cp}$ . Letting  $T_{smp}^{(s)}$  be the sampling interval at the transmitter (where the superscript ‘(s)’ stands for ‘synchronous’), we define  $T_{sc} \triangleq N_{sc}T_{smp}^{(s)}$ ,  $T_{cp} \triangleq N_{cp}T_{smp}^{(s)}$  and  $T_{sym} = T_{sc} + T_{cp}$ . The transmitted complex baseband OFDM signal  $s(t)$  can be expressed as [5, Eqns. (1)-(2)] (the reference time for the phase is set to the end of the CP of each OFDM symbol, see, e.g., [11, Eqn. (1)]):

$$s(t) = \frac{1}{\sqrt{T_{sc}}} \sum_{m=-\infty}^{\infty} \sum_{k=0}^{N_{sc}-1} D_{m,k} e^{j\frac{2\pi k(t-T_{cp}-mT_{sym})}{T_{sc}}} \cdot p(t - mT_{sym}) \quad (2)$$

where the real-valued pulse shaping function  $p(t)$  satisfies  $p(t) = 1$  for  $0 \leq t < T_{sym}$  and  $p(t) = 0$  otherwise. Denoting the channel impulse response (CIR) by  $h(t)$ , the offset between the frequencies of the carrier oscillators at the

transmitter and at the receiver by  $\Delta f$  [Hz], and the sampling time offset (STO) by  $\tau > 0$  [sec], the baseband received channel output signal is expressed as

$$r(t) = (h(t) \star s(t - \tau)) \cdot e^{j2\pi \Delta f t} + w(t), \quad (3)$$

where  $w(t)$  denotes a circularly symmetric proper complex Normal noise process [5]. When the sampling interval at the receiver,  $T_{\text{samp}}^{(a)}$ , is different from that at the transmitter (where the superscript ‘(a)’ stands for ‘asynchronous’), it results in an SFO represented as  $\delta \triangleq \frac{T_{\text{samp}}^{(a)} - T_{\text{samp}}^{(s)}}{T_{\text{samp}}^{(s)}}$ . We denote the CFO at the receiver normalized by the synchronous sampling time,  $T_{\text{samp}}^{(s)}$ , with  $\epsilon \triangleq \Delta f \cdot T_{\text{samp}}^{(s)}$ . In the current model we do not make any additional assumptions on the relationship between the sampling clock and the carrier oscillator. It is noted that there are works which assume that both the sampling clock and the carrier oscillator are generated from a single clock, which induces a deterministic relationship between the SFO and the CFO, see e.g., [12]. Typically, such an assumption is used for motivating further model simplifications, such as neglecting the impact of the the SFO on the phase of the frequency domain representation, see e.g., [12], [13], and [14].

In the current paper, we consider estimation of the residual CFO and SFO, which takes place after coarse acquisition has been applied at the beginning of the reception of the OFDM frame, leaving a relatively small CFO and SFO. Using the approximation  $k\delta + \epsilon + \delta\epsilon \approx \epsilon + k\delta$ , see [5, Sec. II], and further normalizing the CFO  $\epsilon$  by  $N_{\text{sc}}$  to obtain  $\epsilon_n \triangleq N_{\text{sc}}\epsilon$ , where the useful range for residual CFO estimation, denoted  $\mathcal{A}_{\epsilon_n}$ , will be identified explicitly for each estimator in the simulation study in Section V, the received signal in the frequency domain can be expressed as [4, Eqn. (2)]:

$$R_{m,k} = D_{m,k} \tilde{H}_{m,k} \frac{\sin(\pi(\epsilon_n + k\delta))}{N_{\text{sc}} \sin(\frac{\pi(\epsilon_n + k\delta)}{N_{\text{sc}}})} \cdot e^{j\frac{\pi}{N_{\text{sc}}}((N_{\text{sc}}-1)+2N_{\text{cp}}+2mN_{\text{sym}})(\epsilon_n+k\delta)} e^{-j2\pi\frac{\tau}{T_{\text{sc}}}k} + \text{ICI}_{m,k} + W_{m,k}, \quad (4)$$

where  $\text{ICI}_{m,k}$  represents the intercarrier-interference (ICI) at the  $k$ -th subcarrier of the  $m$ -th OFDM symbol and  $W_{m,k} \sim \mathcal{CN}(0, \sigma_W^2)$  represents an i.i.d circularly symmetric complex Normal random process with variance  $\sigma_W^2$ , independent over  $m$  and  $k$ , which results from the application of the DFT to blocks of  $N_{\text{sc}}$  samples of  $w(t)$ , where at each OFDM symbol duration, a single block of  $N_{\text{sc}}$  samples is taken. We observe that the effect of the STO on the frequency domain signal is a different phase offset at each subcarrier  $k$ , which is a function of  $k$  but is independent of  $m$ . Therefore, the impact of the STO can be absorbed into the unknown frequency domain channel coefficients, denoted  $\tilde{H}_{m,k}$ , and we can denote the resulting product by  $H_{m,k} \triangleq \tilde{H}_{m,k} e^{-j2\pi\frac{\tau}{T_{\text{sc}}}k}$ .

From [4, Sec. VI] and [5, Sec. II], it is observed that  $\mathbb{E}\{|\text{ICI}_{m,k}|^2\} \approx \sigma_D^2 |\tilde{H}_{m,k}|^2 \frac{\pi^2 \epsilon_n^2}{3}$ , hence, for values of  $\epsilon_n$  and  $\delta$

relevant to practical scenarios [15], the term  $\text{ICI}_{m,k}$  is negligible compared to the noise term  $W_{m,k}$ : As a numerical example for this point, consider a normalized CFO of  $\epsilon_n \cong 0.02$ , and let  $T_{\text{samp}}^{(a)} = T_{\text{samp}}^{(s)}$ , corresponding to  $\delta = 0$ . Assuming, in addition,  $|\tilde{H}_{m,k}|^2 = 1$ , we obtain  $\mathbb{E}\{|\text{ICI}_{m,k}|^2\} \approx \sigma_D^2 \cdot 1.316 \cdot 10^{-3}$ . Requiring the noise power to be at least 10 times stronger than the ICI power to be able to neglect the ICI, we obtain that for  $\frac{\sigma_D^2}{\sigma_W^2} < 19$  [dB] the ICI can be neglected. This approximation leads to the following approximate received signal model:

$$R_{m,k} \cong D_{m,k} H_{m,k} \Pi_k(\epsilon_n, \delta) e^{j\Theta_{m,k}(\epsilon_n, \delta)} + W_{m,k}, \quad (5)$$

where

$$\begin{aligned} \Pi_k(\epsilon_n, \delta) &= \frac{\sin(\pi(\epsilon_n + k\delta))}{N_{\text{sc}} \sin(\frac{\pi(\epsilon_n + k\delta)}{N_{\text{sc}}})} \\ \Theta_{m,k}(\epsilon_n, \delta) &= \frac{\pi}{N_{\text{sc}}}((N_{\text{sc}} - 1) + 2N_{\text{cp}} + 2mN_{\text{sym}})(\epsilon_n + k\delta). \end{aligned}$$

Note that while the CFO is assumed sufficiently small to allow neglecting the ICI, it still affects the received signal component through the magnitude term  $\Pi_k(\epsilon_n, \delta)$  and, more significantly, through the phase term  $\Theta_{m,k}(\epsilon_n, \delta)$ . Thus, leaving the CFO uncompensated will necessarily result in a degradation in the performance of the OFDM decoder, due to an accumulated phase rotation in the frequency domain, hence CFO estimation absolutely necessary.

### III. LOW COMPLEXITY ESTIMATION ALGORITHM FOR THE SFO AND THE CFO

Begin by rewriting the phase term  $\Theta_{m,k}(\epsilon_n, \delta)$  as:

$$\begin{aligned} \Theta_{m,k}(\epsilon_n, \delta) &= \frac{\pi}{N_{\text{sc}}}(2mN_{\text{sym}} + 2N_{\text{cp}} + N_{\text{sc}} - 1)k\delta \\ &\quad + \frac{\pi}{N_{\text{sc}}}(2mN_{\text{sym}} + 2N_{\text{cp}} + N_{\text{sc}} - 1)\epsilon_n. \end{aligned} \quad (6)$$

Observe that at the  $m$ -th OFDM symbol, the coefficient of the CFO  $\epsilon_n$  is constant over all subcarrier indices  $k$  whereas the coefficient of the SFO  $\delta$  varies linearly with the subcarrier index  $k$ . For sufficiently high SNR we can derive estimators for the SFO and the CFO based on (5) while ignoring the additive noise component of the received signal, via the basic idea of [6]. The impact of the noise will be later evaluated in the simulations study in Section V. The estimators use a set  $\mathcal{K}_p$  of pilot subcarriers, such that  $\mathcal{K}_p$  contains all subcarriers indexes used for pilot transmission. The pilots are embedded into two consecutive OFDM symbols, where it is further assumed that the channel remains constant over two consecutive OFDM symbols. The receiver is assumed to know only the modulator parameters  $N_{\text{sc}}$  and  $N_{\text{cp}}$  as well as the indexes of the pilot subcarriers.

#### A. ESTIMATION OF THE SFO

Consider OFDM symbols  $m$  and  $m + 1$  (we assume the actual value of  $m$  is unknown to the receiver): Assuming the channel vary sufficiently slow such that subcarriers with the same indices experience the same channel coefficients,

we obtain (recall that we ignore  $W_{m,k}$ )

$$\begin{aligned} \frac{R_{m,k}}{R_{m+1,k}} &\cong \frac{D_{m,k}}{D_{m+1,k}} \frac{H_{m,k}}{H_{m+1,k}} \frac{\Pi_k(\epsilon_n, \delta)}{\Pi_k(\epsilon_n, \delta)} \\ &\cdot \frac{e^{j\frac{\pi}{N_{sc}}(2mN_{sym}+2N_{cp}+N_{sc}-1)k\delta}}{e^{j\frac{\pi}{N_{sc}}(2mN_{sym}+2N_{cp}+N_{sc}-1)\epsilon_n}} \\ &\cdot \frac{e^{j\frac{\pi}{N_{sc}}(2mN_{sym}+2N_{cp}+N_{sc}-1)\epsilon_n}}{e^{j\frac{\pi}{N_{sc}}(2mN_{sym}+2N_{cp}+N_{sc}-1)k\delta}} \\ &\stackrel{(a)}{=} \frac{D_{m,k}}{D_{m+1,k}} e^{-j\frac{\pi}{N_{sc}}2N_{sym}k\delta} e^{-j\frac{\pi}{N_{sc}}2N_{sym}\epsilon_n} \end{aligned} \quad (7)$$

where in (a) we used the assumption  $H_{m,k} \cong H_{m+1,k}$ . Consider two subcarrier indices  $k_1$  and  $k_2$ , both belong to  $\mathcal{K}_p$ : From (7) we obtain, after ignoring the noise:

$$\frac{R_{m,k_1}}{R_{m+1,k_1}} \cong \frac{D_{m,k_1}}{D_{m+1,k_1}} \cdot e^{-j2\pi\frac{N_{sym}}{N_{sc}}k_1\delta} \cdot e^{-j2\pi\frac{N_{sym}}{N_{sc}}\epsilon_n} \quad (8a)$$

$$\frac{R_{m,k_2}}{R_{m+1,k_2}} \cong \frac{D_{m,k_2}}{D_{m+1,k_2}} \cdot e^{-j2\pi\frac{N_{sym}}{N_{sc}}k_2\delta} \cdot e^{-j2\pi\frac{N_{sym}}{N_{sc}}\epsilon_n} \quad (8b)$$

Next, define the cost function  $G_{m,k_1,k_2}(\Delta\varphi)$  as follows:

$$\begin{aligned} G_{m,k_1,k_2}(\Delta\varphi) &\triangleq \left| \frac{R_{m,k_1}}{R_{m+1,k_1}} - \frac{R_{m,k_2}}{R_{m+1,k_2}} e^{-j\Delta\varphi} \right|^2 \\ &\cong \left| \frac{D_{m,k_1}}{D_{m+1,k_1}} e^{-j2\pi\frac{N_{sym}}{N_{sc}}k_1\delta} \cdot e^{-j2\pi\frac{N_{sym}}{N_{sc}}\epsilon_n} \right. \\ &\quad \left. - \frac{D_{m,k_2}}{D_{m+1,k_2}} e^{-j\left(2\pi\frac{N_{sym}}{N_{sc}}k_2\delta+\Delta\varphi\right)} e^{-j2\pi\frac{N_{sym}}{N_{sc}}\epsilon_n} \right|^2 \\ &= \left| e^{-j2\pi\frac{N_{sym}}{N_{sc}}\epsilon_n} e^{-j2\pi\frac{N_{sym}}{N_{sc}}k_1\delta} \right. \\ &\quad \left. \cdot \left| \frac{D_{m,k_1}}{D_{m+1,k_1}} - \frac{D_{m,k_2}}{D_{m+1,k_2}} e^{j\left(2\pi\frac{N_{sym}}{N_{sc}}(k_1-k_2)\delta-\Delta\varphi\right)} \right|^2 \right|. \end{aligned} \quad (9)$$

Let constellation symbols at subcarriers  $k_1$  and  $k_2$  of OFDM symbol  $m+1$  be selected such that  $D_{m+1,k_1} = D_{m,k_1}$  and  $D_{m+1,k_2} = D_{m,k_2}$ , i.e.,  $D_{m+1,k_1}$  and  $D_{m+1,k_2}$  can be considered as pilot symbols inserted to facilitate SFO estimation. Therefore,  $\frac{D_{m,k_1}}{D_{m+1,k_1}} = \frac{D_{m,k_2}}{D_{m+1,k_2}}$  and  $G_{m,k_1,k_2}(\Delta\varphi)$  can be expressed as:

$$\begin{aligned} G_{m,k_1,k_2}(\Delta\varphi) &= \left| 1 - e^{j\left(\frac{2\pi}{N_{sc}}N_{sym}(k_1-k_2)\delta-\Delta\varphi\right)} \right|^2 \\ &= 2\left(1 - \cos\left(2\pi\frac{N_{sym}}{N_{sc}}(k_1-k_2)\delta - \Delta\varphi\right)\right). \end{aligned} \quad (10)$$

For  $\Delta\varphi = -\frac{\pi}{2}$  we obtain

$$G_{m,k_1,k_2}\left(-\frac{\pi}{2}\right) = 2\left(1 + \sin\left(2\pi\frac{N_{sym}}{N_{sc}}(k_1-k_2)\delta\right)\right),$$

and for  $\Delta\varphi = \frac{\pi}{2}$  we obtain

$$G_{m,k_1,k_2}\left(\frac{\pi}{2}\right) = 2\left(1 - \sin\left(2\pi\frac{N_{sym}}{N_{sc}}(k_1-k_2)\delta\right)\right),$$

therefore

$$\begin{aligned} \Delta G_{m,k_1,k_2} &= \frac{1}{4}\left(G_{m,k_1,k_2}\left(-\frac{\pi}{2}\right) \right. \\ &\quad \left. - G_{m,k_1,k_2}\left(\frac{\pi}{2}\right)\right) \\ &= \sin\left(2\pi\frac{N_{sym}}{N_{sc}}(k_1-k_2)\delta\right) \end{aligned} \quad (11)$$

It follows that an estimator of the SFO  $\delta$  can be obtained as

$$\hat{\delta}_{k_1,k_2} = \frac{1}{2\pi} \cdot \frac{N_{sc}}{(k_1-k_2)N_{sym}} \cdot \sin^{-1}\left(\Delta G_{m,k_1,k_2}\right). \quad (12)$$

Using the set of pilot subcarriers  $\mathcal{K}_p$ , it follows that the maximal number of pairs of subcarriers which can be used for generating SFO estimates is  $\frac{|\mathcal{K}_p|(|\mathcal{K}_p|-1)}{2}$ , yet it may as well be that the estimator does not need all these pairs, and it uses only a set  $\mathcal{N}_{SFO}$  of pairs of subcarriers,  $1 \leq |\mathcal{N}_{SFO}| \leq \frac{|\mathcal{K}_p|(|\mathcal{K}_p|-1)}{2}$ , to compute estimates, where the output is obtained as the mean of these estimates:

$$\hat{\delta} = \frac{\sum_{(k_1,k_2) \in \mathcal{N}_{SFO}} \hat{\delta}_{k_1,k_2}}{|\mathcal{N}_{SFO}|} \quad (13)$$

where  $\hat{\delta}_{k_1,k_2}$  is an SFO estimate obtained via Eqn. (12).

## B. ESTIMATION OF THE CFO

In this section, we propose two CFO estimators, both of which utilize the estimated  $\hat{\delta}$  for pre-processing the received signal stated in Eqn. (5).

For the first CFO estimator, consider the cost function  $F_{m,k_1}(\Delta\varphi)$  for subcarrier  $k_1 \in \mathcal{K}_p$  (recall that we ignore  $W_{m,k_1}$ ):

$$F_{m,k_1}(\Delta\varphi) \triangleq \left| R_{m+1,k_1} \cdot e^{-j2\pi\frac{N_{sym}}{N_{sc}}k_1\hat{\delta}} \cdot e^{j\Delta\varphi} - R_{m,k_1} \right|^2 \quad (14)$$

Recalling the assumption  $H_{m,k_1} \cong H_{m+1,k_1}$  and the assignment  $D_{m,k_1} = D_{m+1,k_1}$ , we can express  $F_{m,k_1}(\Delta\varphi)$  as:

$$\begin{aligned} F_{m,k_1}(\Delta\varphi) &\cong |H_{m,k_1}|^2 |D_{m,k_1}|^2 |\Pi_{k_1}(\epsilon_n, \delta)|^2 \\ &\quad \cdot \left| e^{j\frac{\pi}{N_{sc}}(2(m+1)N_{sym}+2N_{cp}+N_{sc}-1)(k_1\delta+\epsilon_n)} \right. \\ &\quad \cdot e^{-j2\pi\frac{N_{sym}}{N_{sc}}k_1\hat{\delta}} \cdot e^{j\Delta\varphi} \\ &\quad \left. - e^{j\frac{\pi}{N_{sc}}(2mN_{sym}+2N_{cp}+N_{sc}-1)(k_1\delta+\epsilon_n)} \right|^2 \\ &= |H_{m,k_1}|^2 |D_{m,k_1}|^2 |\Pi_{k_1}(\epsilon_n, \delta)|^2 \\ &\quad \cdot \left| e^{j\frac{\pi}{N_{sc}}(2mN_{sym}+2N_{cp}+N_{sc}-1)(k_1\delta+\epsilon_n)} \right. \\ &\quad \cdot \left| e^{j\left(2\pi\frac{N_{sym}}{N_{sc}}(k_1(\delta-\hat{\delta})+\epsilon_n)+\Delta\varphi\right)} - 1 \right|^2 \\ &\stackrel{(a)}{\cong} 2|H_{m,k_1}|^2 |D_{m,k_1}|^2 |\Pi_{k_1}(\epsilon_n, \delta)|^2 \\ &\quad \cdot \left(1 - \cos\left(2\pi\frac{N_{sym}}{N_{sc}}\epsilon_n + \Delta\varphi\right)\right), \end{aligned} \quad (15)$$

where in (a) we used  $\delta \cong \hat{\delta}$ . Observe that  $\frac{N_{sym}}{N_{sc}} > 1$ . Now, we proceed by obtaining the values of  $F_{m,k_1}(\Delta\varphi)$  at three points: At  $\Delta\varphi = 0$  we have

$$\begin{aligned} F_{m,k_1}(0) &= 2|H_{m,k_1}|^2 |D_{m,k_1}|^2 |\Pi_{k_1}(\epsilon_n, \delta)|^2 \\ &\quad \cdot \left(1 - \cos\left(2\pi\frac{N_{sym}}{N_{sc}}\epsilon_n\right)\right), \end{aligned}$$

at  $\Delta\varphi = -\frac{\pi}{2}$  we obtain

$$\begin{aligned} F_{m,k_1}\left(-\frac{\pi}{2}\right) &= 2|H_{m,k_1}|^2|D_{m,k_1}|^2|\Pi_{k_1}(\epsilon_n, \delta)|^2 \\ &\quad \cdot \left(1 - \cos\left(2\pi\frac{N_{\text{sym}}}{N_{\text{sc}}}\epsilon_n - \frac{\pi}{2}\right)\right) \\ &= 2|H_{m,k_1}|^2|D_{m,k_1}|^2|\Pi_{k_1}(\epsilon_n, \delta)|^2 \\ &\quad \cdot \left(1 - \sin\left(2\pi\frac{N_{\text{sym}}}{N_{\text{sc}}}\epsilon_n\right)\right), \end{aligned}$$

and at  $\Delta\varphi = \pi$  we obtain

$$\begin{aligned} F_{m,k_1}(\pi) &= 2|H_{m,k_1}|^2|D_{m,k_1}|^2|\Pi_{k_1}(\epsilon_n, \delta)|^2 \\ &\quad \cdot \left(1 + \cos\left(2\pi\frac{N_{\text{sym}}}{N_{\text{sc}}}\epsilon_n\right)\right). \end{aligned}$$

Using these quantities we can compute  $F_{m,k_1}^{(I)}$  and  $F_{m,k_1}^{(Q)}$  defined as

$$\begin{aligned} F_{m,k_1}^{(I)} &= F_{m,k_1}(\pi) - F_{m,k_1}(0) \\ &= 4|H_{m,k_1}|^2|D_{m,k_1}|^2|\Pi_{k_1}(\epsilon_n, \delta)|^2 \cdot \cos\left(2\pi\frac{N_{\text{sym}}}{N_{\text{sc}}}\epsilon_n\right) \end{aligned} \quad (16)$$

and

$$\begin{aligned} F_{m,k_1}^{(Q)} &= F_{m,k_1}(\pi) + F_{m,k_1}(0) - 2F_{m,k_1}\left(-\frac{\pi}{2}\right) \\ &= 4|H_{m,k_1}|^2|D_{m,k_1}|^2|\Pi_{k_1}(\epsilon_n, \delta)|^2 \cdot \sin\left(2\pi\frac{N_{\text{sym}}}{N_{\text{sc}}}\epsilon_n\right). \end{aligned} \quad (17)$$

Hence, the first CFO estimator proposed in this work is obtained as:

$$\hat{\epsilon}_{n,k_1}^{(1)} = \frac{1}{2\pi} \cdot \frac{N_{\text{sc}}}{N_{\text{sym}}} \cdot \tan^{-1}\left(\frac{F_{m,k_1}^{(Q)}}{F_{m,k_1}^{(I)}}\right). \quad (18)$$

A second CFO estimator is proposed based on the fraction in Eqn. (7):

$$\frac{R_{m,k_1}}{R_{m+1,k_1}} \cong \frac{D_{m,k_1}}{D_{m+1,k_1}} e^{-j2\pi\frac{N_{\text{sym}}}{N_{\text{sc}}}k_1\delta} e^{-j2\pi\frac{N_{\text{sym}}}{N_{\text{sc}}}\epsilon_n}.$$

Recall that constellation symbols at the  $k_1$ -th subcarriers of OFDM symbols  $m$  and  $m+1$  have been selected such that  $D_{m+1,k_1} = D_{m,k_1}$ . Then, applying the same pre-processing used to obtain the CFO cost function in (14) we arrive at

$$\frac{R_{m,k_1}}{R_{m+1,k_1}} e^{j2\pi\frac{N_{\text{sym}}}{N_{\text{sc}}}k_1\hat{\delta}} \cong e^{-j2\pi\frac{N_{\text{sym}}}{N_{\text{sc}}}k_1(\delta-\hat{\delta})} e^{-j2\pi\frac{N_{\text{sym}}}{N_{\text{sc}}}\epsilon_n}.$$

Assuming successful SFO estimation, i.e.,  $\delta \cong \hat{\delta}$ , we further obtain

$$\frac{R_{m,k_1}}{R_{m+1,k_1}} e^{j2\pi\frac{N_{\text{sym}}}{N_{\text{sc}}}k_1\hat{\delta}} \cong e^{-j2\pi\frac{N_{\text{sym}}}{N_{\text{sc}}}\epsilon_n}$$

and finally, the second CFO estimator is obtained as

$$\hat{\epsilon}_{n,k_1}^{(2)} = -\frac{1}{2\pi} \cdot \frac{N_{\text{sc}}}{N_{\text{sym}}} \cdot \arg\left\{\frac{R_{m,k_1}}{R_{m+1,k_1}} e^{j2\pi\frac{N_{\text{sym}}}{N_{\text{sc}}}k_1\hat{\delta}}\right\} \quad (19)$$

Recalling that the set of pilot subcarriers is  $\mathcal{K}_p$ , then the final estimate with each of the proposed CFO estimators, of Eqn. (18) and of Eqn. (19), is obtained by averaging over the estimates computed for the  $|\mathcal{K}_p|$  pilots, i.e.

$$\hat{\epsilon}_n^{(i)} = \frac{\sum_{k_1 \in \mathcal{K}_p} \hat{\epsilon}_{n,k_1}^{(i)}}{|\mathcal{K}_p|} \quad (20)$$

where  $\hat{\epsilon}_{n,k_1}^{(i)}$ ,  $k_1 \in \mathcal{K}_p$ , are the  $|\mathcal{K}_p|$  CFO estimates obtained via Eqn. (18) or Eqn. (19) for  $i = 1, 2$ , respectively.

### C. SUMMARY: STEPS OF THE SFO AND CFO ESTIMATION ALGORITHM

#### 1) INITIALIZATION

- Let  $\mathcal{K}_p$  be the set of pilot subcarriers.
- Let  $\mathcal{N}_{\text{SFO}}$  be the set of pairs of subcarriers used for SFO estimation.
- Let  $N_{\text{sc}}$  and  $N_{\text{cp}}$  be the number of subcarriers in an OFDM symbol and the length of the CP, respectively.

#### 2) STEPS OF THE ALGORITHM

- 1) The algorithm receives the samples of two subsequent OFDM symbols. Arbitrarily index these symbols as OFDM symbol number  $m$  and OFDM symbol number  $m+1$ , since the actual value of  $m$  does not impact the estimator. For each symbol, the CP is removed and a DFT of size  $N_{\text{sc}}$  is applied.
- 2) For each pair of subcarriers  $(k_1, k_2) \in \mathcal{N}_{\text{SFO}}$ :
  - a) Compute  $G_{m,k_1,k_2}(\Delta\varphi)$  via Eqn. (9) for  $\Delta\varphi = -\frac{\pi}{2}$  and for  $\Delta\varphi = \frac{\pi}{2}$ .
  - b) Estimate  $\hat{\delta}_{k_1,k_2}$  via Eqns. (11)-(12).
  - c) Obtain the final SFO estimate  $\hat{\delta}$  by averaging all  $\hat{\delta}_{k_1,k_2}$ , via Eqn. (13).
- 3) The CFO can now be estimated either via  $\hat{\epsilon}_{n,k_1}^{(1)}$  or via  $\hat{\epsilon}_{n,k_1}^{(2)}$ 
  - For applying CFO estimator  $\hat{\epsilon}_{n,k_1}^{(1)}$  the following steps are taken for each subcarrier  $k_1 \in \mathcal{K}_p$ :
    - a) Using the estimated SFO  $\hat{\delta}$ , compute the cost function  $F_{m,k_1}(\Delta\varphi)$  via Eqn. (14) for  $\Delta\varphi = -\frac{\pi}{2}$ ,  $\Delta\varphi = 0$  and  $\Delta\varphi = \pi$ .
    - b) Use  $F_{m,k_1}(-\frac{\pi}{2})$ ,  $F_{m,k_1}(0)$  and  $F_{m,k_1}(\pi)$  to compute  $F_{m,k_1}^{(I)}$  and  $F_{m,k_1}^{(Q)}$  via Eqns. (16) and (17), respectively.
    - c) Use  $F_{m,k_1}^{(I)}$  and  $F_{m,k_1}^{(Q)}$  to compute  $\hat{\epsilon}_{n,k_1}^{(1)}$  via Eqn. (18).
  - For applying CFO estimator  $\hat{\epsilon}_{n,k_1}^{(2)}$ , use the estimated SFO  $\hat{\delta}$  to compute  $\hat{\epsilon}_{n,k_1}^{(2)}$  via Eqn. (19).
- 4) Obtain the final CFO estimate by averaging the per-subcarrier estimates (obtained either via  $\hat{\epsilon}_{n,k_1}^{(1)}$  or via  $\hat{\epsilon}_{n,k_1}^{(2)}$ ) via Eqn. (20).

#### IV. COMPUTATIONAL COMPLEXITY ANALYSIS OF THE PROPOSED ALGORITHM AND THE REFERENCE ALGORITHMS

In the simulation study in Section V we compare our estimation algorithms with the algorithms presented in [9] and in [10]: The work in [9] proposed a modified version of the conventional least-squares estimator (LSE) of the CFO and the SFO, in which a subset of pilot subcarriers is selected to achieve unbiased SFO and CFO estimates. To compute the estimates, the algorithm first computes the phase differences between the subcarriers from two consecutive OFDM symbols. Then, the LSE computes two summations over these phase differences, from which the SFO and the CFO estimates are finally obtained. This estimator is referred to in this work as the *LSE estimator*. The ML estimation algorithm proposed in [10] does not use pilot symbols. Instead, it uses the phase difference between two FFT windows within a single OFDM symbol, such that one window contains inter-symbol interference (ISI)-free CP samples. In the following, we refer to this window as the *shifted window*. Then, based on the conditional distribution of the shifted window given the synchronized (non-shifted) window, an SFO estimator employing a single dimension grid search is presented in [10, Eqn. (35)]. Subsequently, the CFO is estimated via a closed-form expression [10, Eqn. (33)], which depends on the SFO estimate. The estimator of [10] is referred to in the following as the *LHHYW (Li-Hu-Heng-Yu-Wang) estimator*. Lastly, we note that the work in [10] also presents an approximate estimator for the SFO which avoids the grid search.

#### A. MODIFICATION TO THE CFO ESTIMATOR OF THE LSE METHOD

The CFO estimator proposed in [9, Eqn. (14)] uses the quantity  $\Lambda_1$  in [9, Eqn. (10)], which constrains the selection of pilot subcarrier indexes in order to avoid bias in the estimated parameters. We propose to use the SFO estimator of (13) in order to obtain an unbiased CFO estimate without restricting the pilot subcarrier indexes used by the CFO estimator. To that aim, recall first the result of the summations in [9, Eqn. (10)]:

$$\Lambda_1 = 2\pi N_p \frac{N_{\text{sym}}}{N_{\text{sc}}} \epsilon_n + \sum_{k \in \mathcal{S}} \tilde{w}_{m,k} + 2\pi \frac{N_{\text{sym}}}{N_{\text{sc}}} \delta \sum_{k \in \mathcal{S}} k \quad (21)$$

where  $\tilde{w}_{m,k}$  is the appropriate noise term, which arises in the computation of the argument, as stated after [9, Eqn. (3)], and where  $\mathcal{S}$  is a selected subset of pilot subcarriers, whose cardinality is  $|\mathcal{S}| = N_p$ . As noted in [9], the term  $2\pi \frac{N_{\text{sym}}}{N_{\text{sc}}} \delta \sum_{k \in \mathcal{S}} k$  induces a bias in the LSE CFO and SFO estimates, whose value depends, among others, on  $\delta$ . To avoid this bias, we propose to first estimate the SFO using (13) and then use the estimated SFO  $\hat{\delta}$  to remove the impact of the SFO on the quantity  $Y_{m,k}$ , defined in [9, Eqn. (2)]. Letting  $\tilde{Y}_{m,k}$  denote the processed  $Y_{m,k}$ , we write:

$$\begin{aligned} \tilde{Y}_{m,k} &= R_{m,k}^* R_{m+1,k} \cdot e^{-j2\pi \frac{N_{\text{sym}}}{N_{\text{sc}}} k \hat{\delta}} \\ &\cong |H_{m,k}|^2 |D_{m,k}|^2 e^{j2\pi \frac{N_{\text{sym}}}{N_{\text{sc}}} (\epsilon_n + k \hat{\delta})} e^{-j2\pi \frac{N_{\text{sym}}}{N_{\text{sc}}} k \hat{\delta}} \end{aligned}$$

$$\begin{aligned} &+ \tilde{W}_{m,k} \cdot e^{-j2\pi \frac{N_{\text{sym}}}{N_{\text{sc}}} k \hat{\delta}} \\ &= |H_{m,k}|^2 |D_{m,k}|^2 e^{j2\pi \frac{N_{\text{sym}}}{N_{\text{sc}}} (\epsilon_n + k (\delta - \hat{\delta}))} \\ &+ \tilde{W}_{m,k} \cdot e^{-j2\pi \frac{N_{\text{sym}}}{N_{\text{sc}}} k \hat{\delta}} \end{aligned} \quad (22)$$

where  $\tilde{W}_{m,k}$  is the noise term, which is concluded from [9, Eqn. (3)]. Using  $\tilde{Y}_{m,k}$  instead of  $Y_{m,k}$  in [9, Eqn. (10)], we obtain the following modified expression for  $\Lambda_1$ , denoted  $\tilde{\Lambda}_1$ :

$$\tilde{\Lambda}_1 = 2\pi N_p \frac{N_{\text{sym}}}{N_{\text{sc}}} \epsilon_n + \sum_{k \in \mathcal{S}} \tilde{w}_{m,k} + 2\pi \frac{N_{\text{sym}}}{N_{\text{sc}}} (\delta - \hat{\delta}) \sum_{k \in \mathcal{S}} k \quad (23)$$

where  $\tilde{w}_{m,k}$  is the appropriate noise contribution after the new processing. Assuming successful SFO estimation, i.e.,  $\hat{\delta} \cong \delta$ , it follows the term  $2\pi \frac{N_{\text{sym}}}{N_{\text{sc}}} (\delta - \hat{\delta}) \sum_{k \in \mathcal{S}} k \cong 0$  for any subset of pilot subcarriers. Thus, using  $\tilde{\Lambda}_1$  in the CFO estimator of [9, Eqn. (14)] instead of the original  $\Lambda_1$  defined in [9, Eqn. (10)], we obtain that the CFO estimator is unbiased regardless of the selection of subcarrier indexes. In this work we refer to this method as the *Modified LSE*, and we emphasize that the SFO is estimated via Eqn. (13).

#### B. DETAILED COMPUTATIONAL COMPLEXITY ANALYSIS

In this section we provide a detailed computational complexity analysis for the proposed algorithms. The complexity analysis for the LSE and the LHHYW algorithms is detailed in Appendix A and Appendix B, respectively. We assume that a real division (RD) is implemented iteratively using the Newton-Raphson method, see [16], with  $2i + 1$  real multiplications (RMs) and  $i$  real additions (RAs), where  $i$  represents the number of iterations required to obtain sufficient accuracy.<sup>1</sup> We assume that a complex division (CD) requires 3 RMs, 3 RDs and 3 RAs [17]. Thus, with the RD complexity of [16], the complexity of a CD is  $6i + 6$  RMs and  $3i + 3$  RAs. We also recall that a complex multiplication (CM) requires 4 RMs and 2 RAs. For simplicity, we assume the trigonometric functions  $\sin(\cdot)$ ,  $\cos(\cdot)$ ,  $\sin^{-1}(\cdot)$  and  $\tan^{-1}(\cdot)$  are approximated via a 5<sup>th</sup> order Taylor series expansion, therefore computing the functions  $\sin(\cdot)$ ,  $\sin^{-1}(\cdot)$  and  $\tan^{-1}(\cdot)$ , each requires 5 RMs and 2 RAs, while computing the function  $\cos(\cdot)$  requires 3 RMs and 2 RAs. Lastly, recall that a complex exponent is computed via Euler's formula,  $e^{jx} = \cos(x) + j \sin(x)$ , where  $x \in \mathcal{R}$ , which requires in total 8 RMs and 4 RAs when using the approximated 5<sup>th</sup> order Taylor expansions for  $\sin(x)$  and for  $\cos(x)$ .

We consider first SFO estimation: Assuming that  $|\mathcal{N}_{\text{SFO}}| \geq 1$  pairs of pilot subcarriers are used for estimating  $\delta$ , the final estimate is the mean of the  $|\mathcal{N}_{\text{SFO}}|$  estimated SFOs, where one estimate is generated with each pair. To compute these estimates, we first apply  $|\mathcal{K}_p|$  CDs, requiring  $|\mathcal{K}_p|(6i + 6)$  RMs and  $|\mathcal{K}_p|(3i + 3)$  RAs. Then, for computing

<sup>1</sup>For  $b \in \mathcal{R}$ , the iterative Newton-Raphson division formula for computing  $1/b$  is [16, Eqn. (21)]:  $x_{i+1} = x_i \cdot (2 - b \cdot x_i)$ , where for a sufficient number of iterations one obtains  $x_{i+1} \approx 1/b$ . Note that for computing  $a/b$  for  $a \in \mathcal{R}$  an additional RM is necessary, which is considered in this paper.

the cost function  $G_{m,k_1,k_2}(\Delta\varphi)$  in Eqn. (9) for  $\Delta\varphi = \pi/2$  and for  $\Delta\varphi = -\pi/2$ , we apply for each  $\Delta\varphi$  a computation of a complex subtraction followed by a complex norm at an overall cost of 2 RMs and 3 RAs. Therefore, evaluating the cost function at both  $\Delta\varphi$  values for all  $\hat{\delta}_{k_1,k_2}$  estimates requires  $4|\mathcal{N}_{\text{SFO}}|$  RMs and  $6|\mathcal{N}_{\text{SFO}}|$  RAs. Note that the multiplication by  $e^{-j\Delta\varphi}$  does not incur complexity as it entails a switch between the real and the imaginary parts with possible sign reversals. Next, in Eqn. (11), we apply a real subtraction per SFO estimate, which requires 1 RA, therefore the total complexity for Eqn. (11) is  $|\mathcal{N}_{\text{SFO}}|$  RAs. Note that the division by 4 does not require RMs or RAs since we assume it is implemented via a shift. Subsequently, in Eqn. (12), the inverse sine,  $\sin^{-1}(\cdot)$ , is computed, which requires 5 RMs and 2 RAs, followed by a real multiplication by a constant. Accordingly, the overall complexity of Eqn. (12) for all  $\hat{\delta}_{k_1,k_2}$  estimates is  $6|\mathcal{N}_{\text{SFO}}|$  RMs and  $2|\mathcal{N}_{\text{SFO}}|$  RAs. Note that we assume the constant,  $N_{\text{sc}}/(2\pi(k_1 - k_2)N_{\text{sym}})$ , used in Eqn. (12), was a-priori computed. The overall complexity for computing  $|\mathcal{N}_{\text{SFO}}|$  SFO estimates is  $|\mathcal{K}_p|(6i + 6) + 10|\mathcal{N}_{\text{SFO}}|$  RMs and  $|\mathcal{K}_p|(3i + 3) + 9|\mathcal{N}_{\text{SFO}}|$  RAs. The estimator outputs the mean of the estimates via Eqn. (13) bringing the total complexity of the SFO estimation to  $|\mathcal{K}_p|(6i + 6) + 10|\mathcal{N}_{\text{SFO}}| + 1$  RMs and  $|\mathcal{K}_p|(3i + 3) + 10|\mathcal{N}_{\text{SFO}}| - 1$  RAs.

Next, consider CFO estimation via the three proposed CFO estimators. Consider first the estimator  $\hat{\epsilon}_{n,k_1}^{(1)}$ , stated in Eqn. (18), and recall that the CFO estimate is obtained by averaging over the  $|\mathcal{K}_p|$   $\hat{\epsilon}_{n,k}^{(1)}$  estimates computed via Eqn. (18), as specified in Eqn. (20). To compute each of the  $|\mathcal{K}_p|$  estimates  $\hat{\epsilon}_{n,k_1}^{(1)}$ , we first apply a real multiplication to obtain the argument of the exponent in Eqn. (14),  $e^{-j2\pi \frac{N_{\text{sym}}}{N_{\text{sc}}} k_1 \hat{\delta}}$ , in which the SFO estimate is multiplied by a constant at an overall cost of  $|\mathcal{K}_p|$  RMs. Note that we assume the constants,  $2\pi N_{\text{sym}} k_1 / N_{\text{sc}}$ , in the argument of the exponent in Eqn. (14) have already been computed. Then, we apply a multiplication of  $R_{m+1,k_1}$  by the complex exponent  $e^{-j2\pi \frac{N_{\text{sym}}}{N_{\text{sc}}} k_1 \hat{\delta}}$ , for which the exponent is expressed in Cartesian form using Euler's formula. Subsequently, for each of the three phase shift values  $\Delta\varphi = 0, \pi/2$  and  $\Delta\varphi = \pi$ , we apply a complex subtraction and a complex norm. The overall complexity for computing (14) for all  $|\mathcal{K}_p|$  pilot subcarriers and the three phase shifts is  $18|\mathcal{K}_p|$  RMs and  $15|\mathcal{K}_p|$  RAs. Note that the multiplication by  $e^{j\Delta\varphi}$  does not incur complexity as it entails a possible switch between the real and the imaginary parts with possible sign reversals. Next, in Eqns. (16) and (17), we apply two real subtractions and one real addition, therefore, the total complexity of this step for all  $|\mathcal{K}_p|$  estimates is  $3|\mathcal{K}_p|$  RAs. Note that we do not account for the multiplication by 2 in Eqn. (17) since we assume that it is implemented via a shift. Subsequently, the CFO estimator of  $\hat{\epsilon}_{n,k_1}^{(1)}$  in Eqn. (18) applies a real division ( $(2i + 1)$  RMs,  $i$  RAs), an inverse tangent,  $\tan^{-1}(\cdot)$  (5 RMs, 2 RAs), followed by a multiplication by a constant. Accordingly, the overall complexity is  $|\mathcal{K}_p|(2i + 7)$  RMs and  $|\mathcal{K}_p|(i + 2)$  RAs. Note that the constant,  $N_{\text{sc}}/(2\pi N_{\text{sym}})$ , has been a-priori computed.

The overall complexity for obtaining  $|\mathcal{K}_p|$  estimates  $\hat{\epsilon}_{n,k_1}^{(1)}$  is  $|\mathcal{K}_p|(2i + 26)$  RMs and  $|\mathcal{K}_p|(i + 20)$  RAs, and the complexity of the output CFO estimate obtained by averaging the  $|\mathcal{K}_p|$   $\hat{\epsilon}_{n,k_1}^{(1)}$  estimates via Eqn. (20) to achieve the final CFO estimate  $\epsilon_n^{(1)}$  is  $|\mathcal{K}_p|(2i + 26) + 1$  RMs and  $|\mathcal{K}_p|(i + 21) - 1$  RAs.

Next, we analyze the computational complexity of the second CFO estimator,  $\hat{\epsilon}_{n,k_1}^{(2)}$ , stated in Eqn. (19). Note that the divisions  $R_{m,k_1}/R_{m+1,k_1}$  do not incur a cost in computational complexity, since they have already been computed at the SFO estimation step, see Eqn. (9). Next, note that  $\arg \left\{ \frac{R_{m,k_1}}{R_{m+1,k_1}} e^{j2\pi \frac{N_{\text{sym}}}{N_{\text{sc}}} k_1 \hat{\delta}} \right\} = \arg \left\{ \frac{R_{m,k_1}}{R_{m+1,k_1}} \right\} + 2\pi \frac{N_{\text{sym}}}{N_{\text{sc}}} k_1 \hat{\delta}$ , and that the CFO estimate is given by Eqn. (20):

$$\begin{aligned} \epsilon_n^{(2)} &= \frac{1}{|\mathcal{K}_p|} \sum_{k_1 \in \mathcal{K}_p} \left( -\frac{1}{2\pi} \frac{N_{\text{sc}}}{N_{\text{sym}}} \right) \\ &\quad \cdot \arg \left\{ \frac{R_{m,k_1}}{R_{m+1,k_1}} e^{j2\pi \frac{N_{\text{sym}}}{N_{\text{sc}}} k_1 \hat{\delta}} \right\} \\ &= -\frac{1}{2\pi} \frac{N_{\text{sc}}}{N_{\text{sym}} |\mathcal{K}_p|} \left( \sum_{k_1 \in \mathcal{K}_p} \arg \left\{ \frac{R_{m,k_1}}{R_{m+1,k_1}} \right\} \right) \\ &\quad + 2\pi \frac{N_{\text{sym}}}{N_{\text{sc}}} \left( \sum_{k_1 \in \mathcal{K}_p} k_1 \right) \hat{\delta}. \end{aligned}$$

Thus, the estimate can be computed by taking  $|\mathcal{K}_p|$  arguments, each requires an RD ( $(2i + 1)$  RMs,  $i$  RAs) and  $\tan^{-1}(\cdot)$  (5 RMs, 2 RAs) at a total complexity of  $|\mathcal{K}_p|(2i + 6)$  RMs and  $|\mathcal{K}_p|(i + 2)$  RAs. Then, the SFO estimate  $\hat{\delta}$  is multiplied by a constant  $2\pi \frac{N_{\text{sym}}}{N_{\text{sc}}} \left( \sum_{k_1 \in \mathcal{K}_p} k_1 \right)$  at a cost of 1 RM and summed with  $|\mathcal{K}_p|$  arguments, bringing the total complexity to  $|\mathcal{K}_p|(2i + 6) + 1$  RMs and  $|\mathcal{K}_p|(i + 3)$  RAs. Finally, an RM is applied to compute the final CFO estimate resulting in a total of  $|\mathcal{K}_p|(2i + 6) + 2$  RMs and  $|\mathcal{K}_p|(i + 3)$  RAs.

Lastly, we analyze the computational complexity of the modified LSE method presented in Sec. IV-A. To compute the CFO estimate, we compute  $\arg \{ \tilde{Y}_{m,k} \} = \arg \left\{ R_{m,k}^* R_{m+1,k} e^{-j2\pi \frac{N_{\text{sym}}}{N_{\text{sc}}} k \hat{\delta}} \right\} = \arg \{ R_{m,k}^* R_{m+1,k} \} - 2\pi \frac{N_{\text{sym}}}{N_{\text{sc}}} k \hat{\delta}$ . Then, we compute the summation term  $\tilde{\Lambda}_1$  in Eqn. (23),  $\tilde{\Lambda}_1 = \sum_{k \in \mathcal{K}_p} \arg \{ \tilde{Y}_{m,k} \} = \sum_{k \in \mathcal{K}_p} \arg \{ R_{m,k}^* R_{m+1,k} \} - 2\pi \frac{N_{\text{sym}}}{N_{\text{sc}}} \hat{\delta} \sum_{k \in \mathcal{K}_p} k$ . To that aim, we first compute  $\arg \{ R_{m,k}^* R_{m+1,k} \}$  using complex multiplication (4 RMs, 2 RAs), real division ( $(2i + 1)$  RMs,  $i$  RAs) and  $\tan^{-1}(\cdot)$  (5 RMs, 2 RAs). The overall complexity of computing  $|\mathcal{K}_p|$  arguments is  $|\mathcal{K}_p|(2i + 10)$  RMs and  $|\mathcal{K}_p|(i + 4)$  RAs. Then, the  $|\mathcal{K}_p|$  arguments are summed at a complexity of 0 RMs and  $|\mathcal{K}_p| - 1$  RAs, and, assuming the term  $2\pi \frac{N_{\text{sym}}}{N_{\text{sc}}} \sum_{k \in \mathcal{K}_p} k$  has been a-priori computed, it follows that computing the term  $\left( 2\pi \frac{N_{\text{sym}}}{N_{\text{sc}}} \sum_{k \in \mathcal{K}_p} k \right) \hat{\delta}$  takes 1 RM. Eventually the latter term is added to the sum of the arguments at a complexity of 0 RMs and 1 RA. Lastly, obtaining the CFO estimate via [9, Eqn. (14)] requires 1 RM, assuming the constant  $N_{\text{sc}}/(2\pi N_{\text{sym}} |\mathcal{K}_p|)$  has already been computed.

Thus, the total complexity is  $|\mathcal{K}_p|(2i + 10) + 2$  RMs and  $|\mathcal{K}_p|(i + 5)$  RAs.

## V. NUMERICAL PERFORMANCE EVALUATION

### A. SIMULATION PARAMETERS

The performance of the estimation algorithms presented in this work are evaluated for communications with parameters corresponding to the IEEE 802.11ax standard operating with a 20 MHz transmission bandwidth at the 2.4 GHz band [18, Sec. III]: The number of subcarriers is set to  $N_{sc} = 256$ , and the CP is set to  $N_{cp} = 32$  samples, which results in  $N_{sym} = 288$  for a single OFDM symbol; Indexing the subcarriers of an OFDM symbol by  $\{0, 1, 2, \dots, 255\}$ , the set of pilot subcarriers is selected for each scheme to maintain approximately the same complexity, as detailed later. We assume a slowly varying frequency selective fading channel with a maximum delay spread of  $T_{ch} = 1050$  [nsec] and a Rician factor of  $K = 6$  [dB] such that the channel remains (approximately) constant over two consecutive transmitted OFDM symbols. In the simulations, we investigate the performance of the algorithms for two different channel realizations, denoted CH1<sup>2</sup> and CH2.<sup>3</sup> We let the data and the pilot symbols be drawn from a quadrature phase-shift keying (QPSK) constellation. For the baseline scenario we use a normalized residual CFO of  $\epsilon_n = 0.01$  and a normalized SFO of  $\delta = 2 \cdot 10^{-4}$ , which corresponds to 200 [ppm]. These residual CFO and SFO values are in line with the values used in previous works.<sup>4</sup> We note that typically, the residual CFO considered in CFO synchronization works is taken to be smaller than half the subcarrier spacing, [19, Section II], [12], [13]. For the simulation scenario parameters used in this section, this corresponds to a maximal CFO of  $\epsilon_n^{\max} = 0.5$ . Therefore, in the numerical evaluation we also test estimators' performance over this entire range. The estimation of the CFO and the SFO is based on two consecutive OFDM symbols. For each data point in the figures, we carried out

<sup>2</sup>The taps for the channel CH1 are  $\mathbf{H} = [0.1946 + 0.0122j, 0.0837 + 0.1256j, -0.1152 - 0.0816j, 0.0719 - 0.3107j, 0.1711 + 0.0297j, -0.0833 + 0.3317j, -0.2358 - 0.116j, -0.07668 - 0.4499j, 0.2839 - 0.1825j, 0.3178 + 0.0873j, 0.0048 + 0.2977j, -0.1350 + 0.1747j, -0.1132 - 0.0077j, -0.0178 - 0.0346j, 0.0643 + 0.0457j, 0.0296 + 0.0436j, -0.0609 - 0.0362j, -0.0448 - 0.0333j, -0.002 - 0.0134j, -0.0052 + 0.0195j, 0.0115 + 0.0065j, 0.0000 + 0.0053j, -0.005 + 0.0131j, -0.0046 + 0.0000j, -0.0036 - 0.0056j, 0.0072 + 0.0026j, 0.0055 + 0.0011j, 0.0008 + 0.0015j]^T$ . Note that  $|\mathbf{H}|^2 = 1$ .

<sup>3</sup>The taps for the channel CH2 are  $\mathbf{H} = [0.0022 + 0.0060j, -0.0059 - 0.0093j, 0.0111 + 0.0140j, -0.0179 - 0.0194j, 0.0267 + 0.0263j, -0.0419 - 0.0407j, 0.0763 + 0.0839j, 0.2135 + 0.0670j, 0.0009 - 0.6324j, 0.0155 + 0.0985j, -0.0361 + 0.4056j, 0.1087 - 0.0703j, 0.1055 + 0.2581j, -0.1558 - 0.2530j, -0.0433 - 0.0254j, 0.3096 + 0.1242j, 0.0174 - 0.0002j, 0.0527 - 0.0985j, -0.0063 + 0.0219j, -0.0555 + 0.1701j, -0.0004 + 0.0141j, -0.0099 - 0.0320j, -0.0337 - 0.0419j, 0.0203 + 0.0087j, -0.0394 + 0.0017j, -0.0509 + 0.0160j, 0.0131 - 0.0059j, -0.0069 + 0.0034j, 0.0140 - 0.0622j, -0.0028 + 0.0013j, 0.0020 - 0.0004j, -0.0012 + 0.0003j]^T$ . Note that  $|\mathbf{H}|^2 = 1$ .

<sup>4</sup>In [4] the CFO used in the simulations is  $\epsilon_n \approx 0.02$  and  $\delta$  corresponds to 100 [ppm]; in [5]  $\delta$  corresponds to 100 [ppm] and  $\epsilon_n = 0.02$ ; in [9] the simulations are carried out for  $\epsilon_n = 0.02$  with  $\delta$  corresponding to 20 [ppm] and for  $\epsilon_n = 0.08$  with  $\delta$  corresponding to 80 [ppm]; and lastly, in [10]  $\epsilon_n = 0.112$  is used while  $\delta$  corresponds to 30 [ppm].

10000 Monte-Carlo experiments. We define the signal-to-noise (SNR) as  $\text{SNR} \triangleq \frac{|H_{m,k}|^2 |\Pi(\epsilon_n, \delta)|^2 \sigma_D^2}{\mathbb{E}\{|W_{m,k}|^2\}}$  and the SNR-per-bit  $E_b/N_0 \triangleq \frac{\text{SNR}}{\log_2(M)}$  where the cardinality of the QPSK constellation set is  $M = 4$ . The received signal is subject to an unknown STO of  $\tau = 100$  [nsec].

In the simulations we compare the proposed estimators with the LSE and with the LHHYW estimator. For the proposed estimators we use pilot subcarriers  $\mathcal{K}_p^{\text{proposed}} = \{49, 238\}$  for estimating the SFO and the CFO, i.e.,  $|\mathcal{K}_p^{\text{proposed}}| = 2$ . To maintain the same computational complexity for all algorithms, the LHHYW estimator uses  $K = 14$  subcarrier indices, which correspond to subcarrier frequency indexes  $\mathcal{K} = \{121, \dots, 127, 129, \dots, 135\}$  for estimating the SFO and the CFO with a single dimensional search applied to the SFO estimation. The search resolution for the SFO estimator is  $\Delta\delta = 2 \cdot 10^{-5}$  and we evaluate the cost at 500 grid search points around the true  $\delta$ , with  $L = 8$ . The LSE of [9] is implemented using a symmetric subset of 6 pilot subcarriers  $\mathcal{K}_p^{\text{LSE}} = \{17, 49, 127, 129, 207, 238\}$  in the set of subcarriers  $\{0, 1, \dots, 254, 255\}$ , to avoid possible bias of the estimates. We note that since the LSE and the LHHYW algorithms are derived assuming the set of subcarrier indexes is symmetric around 0, then for computing these estimates we mapped the set of pilot indexes of the LSE,  $\mathcal{K}_p^{\text{LSE}}$ , and the set of subcarrier indexes of the LHHYW,  $\mathcal{K}$ , to the appropriate values by subtracting 128 from the values of the indexes.

### B. SIMULATION RESULTS

The performance of the proposed estimators as well as of the baseline estimators of [9] and [10] are compared in terms of the mean-squared error (MSE), defined as  $\text{MSE}(\delta) \triangleq \mathbb{E}\{(\delta - \hat{\delta})^2\}$  and  $\text{MSE}(\epsilon_n) \triangleq \mathbb{E}\{(\epsilon_n - \hat{\epsilon}_n)^2\}$ . The MSE plots also depict the Cramer-Rao lower bound (CRB) which is an inherent lower bound on the MSE of the estimated SFO and CFO, see [5]. The CRB expressions are obtained from [5, Eqn. (9)], which specify the CRB for the case of an unknown CIR. We note that in [5] the received model [5, Eqn. (4)] uses the approximation  $\Pi_k(\epsilon_n, \delta) \approx 1$ , which is appropriate also for the current setup (although it is not required by the estimation schemes). Fig. 1 and Fig. 2 depict  $\text{MSE}(\delta)$  versus  $E_b/N_0$  for CH1 and for CH2, respectively, for the proposed SFO estimator of Eqn. (13), the LSE and the LHHYW, as well as the corresponding CRB. We observe in Fig. 1 that the proposed algorithm achieves the smallest MSE while in Fig. 2 the LSE achieves the smallest MSE. Note that in both Figs. 1 and 2 the LHHYW performs very poorly, as the number of subcarriers it uses for estimating the SFO, set to maintain fairness of comparison, is not sufficient for this algorithm to achieve a small MSE. We also observe that none of the algorithms approaches the CRB, which is expected as the algorithms use a very small number of symbols (2 OFDM symbols) and a small number of pilot subcarriers, hence asymptotic conditions required for obtaining the CRB are not satisfied. Moreover, the focus in the current algorithms

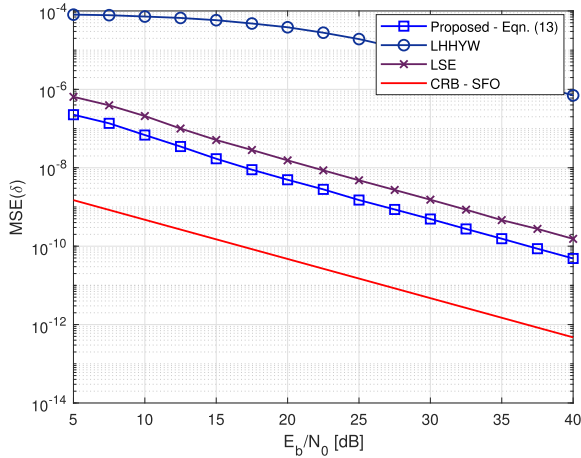


FIGURE 1.  $MSE(\delta)$  vs.  $E_b/N_0$  with  $\epsilon_n = 0.01$  and  $\delta = 2 \cdot 10^{-4}$  for CH1.

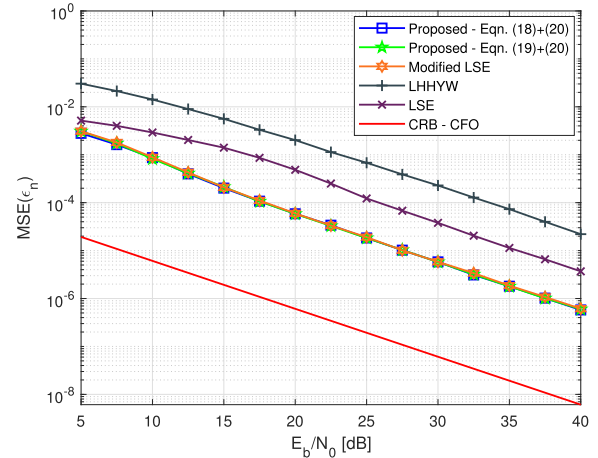


FIGURE 3.  $MSE(\epsilon_n)$  vs.  $E_b/N_0$  with  $\epsilon_n = 0.01$  and  $\delta = 2 \cdot 10^{-4}$  for CH1.

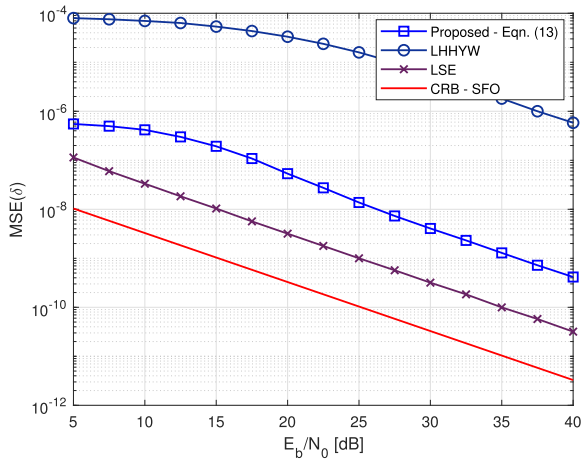


FIGURE 2.  $MSE(\delta)$  vs.  $E_b/N_0$  with  $\epsilon_n = 0.01$  and  $\delta = 2 \cdot 10^{-4}$  for CH2.

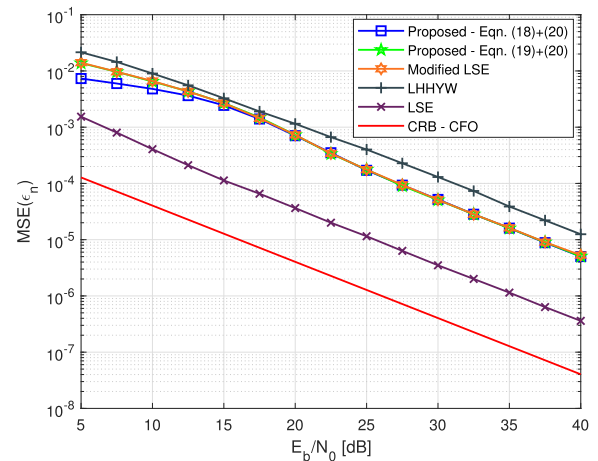


FIGURE 4.  $MSE(\epsilon_n)$  vs.  $E_b/N_0$  with  $\epsilon_n = 0.01$  and  $\delta = 2 \cdot 10^{-4}$  for CH2.

is on good performance at low computational complexity and not on the asymptotic case, thus, the goal is to obtain performance improvement compared to previously proposed schemes, which is indeed achieved by the current work.

Figs. 3 and 4 depict  $MSE(\epsilon_n)$  versus  $E_b/N_0$  for CH1 and for CH2, respectively, as well as the corresponding CRB. In both figures,  $\hat{\epsilon}_n^{(1)}$ , is referred to as ‘Proposed - Eqn. (18) + (20)’, and  $\hat{\epsilon}_n^{(2)}$ , is referred to as ‘Proposed - Eqn. (19) + (20)’; Both  $\hat{\epsilon}_n^{(1)}$  and  $\hat{\epsilon}_n^{(2)}$  use the estimated  $\hat{\delta}$  obtained via Eqn. (13). Comparison also includes the modified LSE, the LSE and the LHHYW CFO estimators. Observe that for CH1, the two proposed CFO estimators and the modified LSE achieve a smaller MSE than the LSE and the LHHYW while for CH2 the LSE achieves a smaller MSE compared to the proposed CFO estimators. The LHHYW achieves the worst performance in both CH1 and CH2, which is expected as its CFO estimate depends on its SFO estimate, which has a poor performance as shown in Figs. 1 and 2. Note that also here, the estimators do not attain the CRB due to their suboptimal processing as well as the distance from the asymptotic situation.

It follows from the SFO and the CFO estimation results in Figs. 2 and 4 that for CH2, the LSE algorithm achieves a lower MSE than the proposed algorithms. This is explained by noting that the LSE algorithm relies on *phase* computation while the proposed algorithms have a stronger dependence on the *magnitude* of the subcarriers as they apply a complex division. The difference in estimators’ performance for the two channels follows by observing the magnitudes of the discrete-time Fourier transforms (DTFTs) of the CIRs for CH1 and for CH2 at the pilot subcarriers used by the proposed estimators, marked with the red circles in Fig. 5. Observe that the magnitudes of the pilot subcarriers are stronger in CH1 compared to CH2, hence the superior performance of the proposed estimators in CH1.

Next we study the impact of the value of the normalized CFO on the CFO estimation performance. To that aim we considered a residual SFO of  $\delta = 2 \cdot 10^{-4}$  at  $E_b/N_0 = 15$  [dB], and depict the MSE vs.  $\epsilon_n$  in Fig. 6, and the mean estimate vs.  $\epsilon_n$  in Fig. 7, for  $\epsilon_n \in [-0.5, 0.5)$ . Note that as the results are symmetric around  $\epsilon_n = 0$ , than Fig. 6 depicts MSE only for the positive half of the range of  $\epsilon_n$ . It is observed

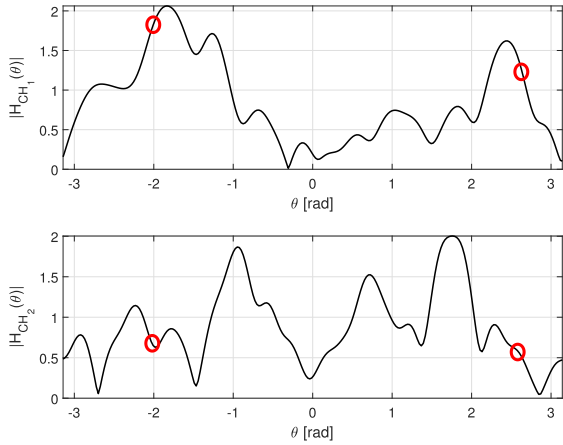


FIGURE 5. Magnitude of the DTFT of the CIR for CH1 (top) and for CH2 (bottom). The circles mark the subcarriers used by the proposed estimators.

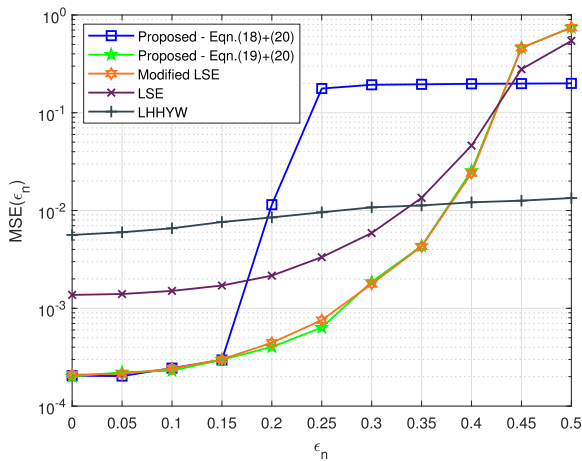


FIGURE 6. MSE of the CFO estimates vs. the value of the normalized CFO with  $\delta = 2 \cdot 10^{-4}$  for CH1, at  $E_b/N_0 = 15$  [dB].

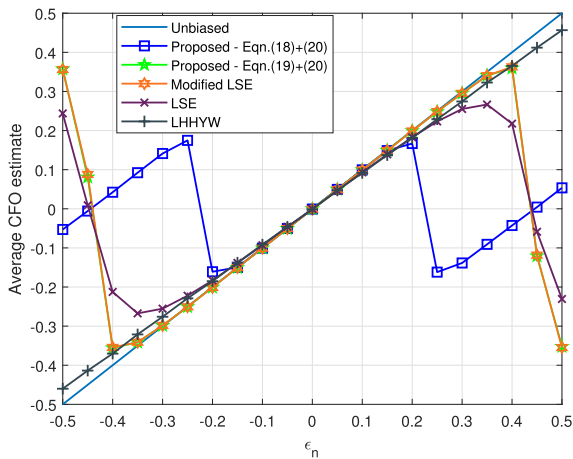


FIGURE 7. Mean of the CFO estimates vs. the value of the normalized CFO with  $\delta = 2 \cdot 10^{-4}$  for CH1, at  $E_b/N_0 = 15$  [dB].

from the figures that, for the given scenario, the proposed CFO estimator  $\hat{\epsilon}_n^{(2)}$  of Eqns. (19) + (20) and the modified LSE of Section IV-A are useful (here we refer to usefulness as having a relatively small bias and no jump in MSE) in the range  $\epsilon_n \in [-0.4, 0.4]$ , the CFO estimator of the LSE

has a useful range of  $\epsilon_n \in [-0.35, 0.35]$ , the proposed CFO estimator  $\hat{\epsilon}_n^{(1)}$  of Eqns. (18) + (20) has a useful range of  $\epsilon_n \in [-0.15, 0.15]$ , and the LHYYW CFO estimator has a useful range of  $\epsilon_n \in [-0.5, 0.5]$ . It is also observed from Fig. 6 that the MSE of  $\hat{\epsilon}_n^{(2)}$  and of the modified LSE at  $\epsilon_n = 0.01$  and at  $\epsilon_n = 0.35$  differ by a factor smaller than 15, while the value of  $\epsilon_n$  is increased by a factor of 35 in this range, implying the *relative MSE has decreased* as  $\epsilon_n$  has increased. We also repeated the simulations for  $E_b/N_0 = 10$  [dB], and observed that contrary to the situation for  $E_b/N_0 = 15$  [dB], the CFO estimators of the LSE and the LHYYW exhibit a bias also for small normalized CFOs, e.g., in the range  $[-0.05, 0.05]$ . Note that the bias of the LSE estimator is *not* due to the term from [9, Eqn. (10)]:  $2\pi \frac{N_{\text{sym}}}{N_{\text{sc}}} \delta \sum_{k \in \mathcal{K}_p^{\text{LSE}}} k$ , since the pilot subcarriers were selected a-priori to guarantee  $\sum_{k \in \mathcal{K}_p^{\text{LSE}}} k = 0$ . Hence, the LSE estimator bias may be inherent. The LHYYW bias may be due to its poor SFO estimate which might directly affect the corresponding CFO estimate. It was also verified that all SFO estimators are unbiased (the last two simulations are not included here for brevity). It thus follows that the proposed estimators *are useful over a large range of residual CFO values*, and in particular,  $\hat{\epsilon}_n^{(2)}$  is useful over nearly the entire relevant range of residual CFOs, and its combination with the proposed SFO estimator results in an excellent candidate for joint residual CFO and SFO estimation in many OFDM scenarios.

Comparing Figs. 1, 2, 3 and 4, it follows that there are channels in which the new SFO and CFO estimators are superior to that of the LSE, e.g., CH1 used in Figs. 1 and 3, while there are channels in which the opposite is true. To better understand this points, we carried out a simulation in which we used the built-in MATLAB function ‘wlanTGaxChannel’ from the ‘WLAN System Toolbox’ to generate random channels specifically for the IEEE 802.11ax system, setting the parameters ‘DelayProfile’ to ‘Model-F’, ‘ChannelBandwidth’ to ‘CBW20’, ‘NormalizeChannelOutputs’ to 1, ‘NormalizePathGains’ to 1 and ‘SampleRate’ to  $1/T_{\text{samp}}^{(a)} \cong 19.96$  [MHz]. For the numerical evaluation we generated 11000 random channel realizations, and for each channel realization we tested the performance at three values of  $E_b/N_0 = \{5, 25, 45\}$  [dB], where at each  $E_b/N_0$  we carried out 1000 Monte-Carlo experiments to measure the MSE of the SFO estimate and of the CFO estimate for both the proposed estimators as well as for the LSE estimator. In order to identify which estimator is superior we used a majority rule. From this test we observe that the proposed SFO estimator was superior to the LSE in 57% of the realizations, while the proposed CFO estimators were superior to the LSE, in about half the realizations at which the proposed SFO estimator was superior to the LSE. We can conclude that the proposed CFO estimator is more sensitive to pilot subcarriers selection while the SFO estimator is more robust, and that neither algorithms in uniformly superior. If thus seems that a combination of both the LSE and the proposed algorithms could be the best approach.

TABLE 1. Comparison of the computational complexity.

	Proposed SFO and CFO ( $\hat{\epsilon}_n^{(1)}$ )	Proposed SFO and CFO ( $\hat{\epsilon}_n^{(2)}$ )	Modified LSE	LSE	LHHYW*
RA	$ \mathcal{K}_p (4i + 24) + 10 \mathcal{N}_{\text{SFO}}  - 2$	$ \mathcal{K}_p (4i + 6) + 10 \mathcal{N}_{\text{SFO}}  - 1$	$ \mathcal{K}_p (4i + 8) + 10 \mathcal{N}_{\text{SFO}}  - 1$	$ \mathcal{K}_p (i + 6) - 2$	$6K + 2i + 2$
RM	$ \mathcal{K}_p (8i + 32) + 10 \mathcal{N}_{\text{SFO}}  + 2$	$ \mathcal{K}_p (8i + 12) + 10 \mathcal{N}_{\text{SFO}}  + 3$	$ \mathcal{K}_p (8i + 16) + 10 \mathcal{N}_{\text{SFO}}  + 3$	$ \mathcal{K}_p (2i + 11) + 2$	$8K + 4i + 10$

\*Note that for LHHYW method, the computational complexity is for a single grid search point.

Lastly, as the performance of communications systems are predominantly measured via bit error-rate (BER) at the receiver, it is of interest to characterize the BER performance resulting from applying the different algorithms. Fig. 8 depicts the BER results vs.  $E_b/N_0$  for uncoded QPSK transmission over CH1. The estimation of the SFO and the CFO is applied while the coefficients of CH1 are unknown, but at the symbol decoding step it was assumed that the coefficients of CH1 are known exactly by the decoder. The BER plot for the maximum likelihood symbol decoder over an additive white Gaussian noise (AWGN) channel with the SFO and the CFO completely compensated is included as a reference for comparison (labeled as ‘Ideal’). It can be observed the two proposed estimators and the modified LSE achieve lower BER than the LSE and the LHHYW estimators. This is expected, since the two proposed estimators and the modified LSE achieve lower CFO and SFO MSEs than the LSE and the LHHYW estimators for CH1, as observed in Figs. 1 and 3. It can be observed that above  $E_b/N_0 = 8$  [dB] the two proposed estimators and the modified LSE BER curves practically coincide with the BER curve of the maximum likelihood symbol detector, which demonstrates the superiority of the proposed estimators over the LSE and the LHHYW estimators for CH1. We observe that the larger the MSE in SFO and CFO estimators the higher is BER, which is also as expected. For completeness, we depict the BER performance for CH2 in Fig. 9. We observe from Fig. 9 that for CH2, the BER plot is mirroring the observations from Fig. 8: The BER with both the proposed estimators and the LSE decrease as the SNR increases, and because the LSE has a smaller SFO and CFO MSEs compared to the proposed estimators, then its corresponding BER values are smaller than the BER values obtained with the proposed estimators. It is also observed that as the SNR increases, then eventually the MSE of proposed estimators is sufficiently small such that their BER curves approach the BER curve obtained with the LSE.

C. COMPARISON OF COMPUTATIONAL COMPLEXITY AND A-PRIORI INFORMATION

From the numerical performance evaluations, we note that there are scenarios in which the proposed SFO and the CFO estimators achieve superior MSE performance as depicted in Figs. 1 and 3, while there are scenarios in which the LSE algorithm achieves lower MSE as depicted in Figs. 2 and 4. In order to make a fair and complete comparison of the different algorithms, it is necessary to consider their computational complexity. Table 1 summarizes the computational complexity of the algorithms in terms of RMs and RAs. The LHHYW algorithm uses a grid search, hence its

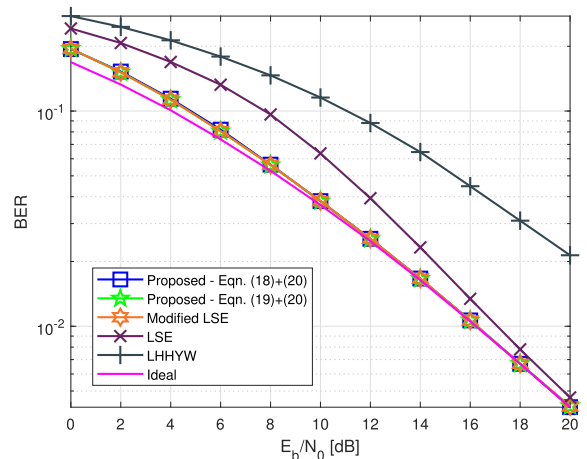


FIGURE 8. BER vs.  $E_b/N_0$  with  $\epsilon_n = 0.01$  and  $\delta = 2 \cdot 10^{-4}$  for CH1.

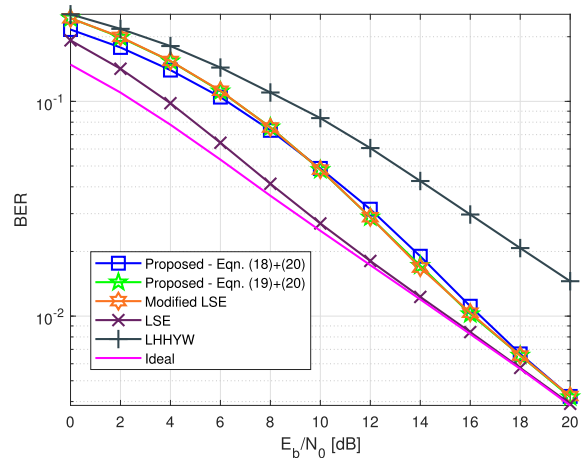


FIGURE 9. BER vs.  $E_b/N_0$  with  $\epsilon_n = 0.01$  and  $\delta = 2 \cdot 10^{-4}$  for CH2.

complexity is stated per grid search point. Note that the proposed approximated version of the SFO estimator presented in [10, Eqn. (37)] does not require a grid search, however its computational complexity in terms of RMs and RAs remains very high for the considered scenario, therefore, we implemented the single dimension grid search SFO estimator [10, Eqn. (35)]. The complexity evaluation for [10, Eqn. (37)] is briefly summarized in Appendix B.

We compare the computational complexity of the different estimation methods via the required number of RMs, as multiplications dominate the computational complexity [20]. From Table 1, we note that the complexity of the LSE has a linear dependence on  $|\mathcal{K}_p|$ , while the complexity of the proposed

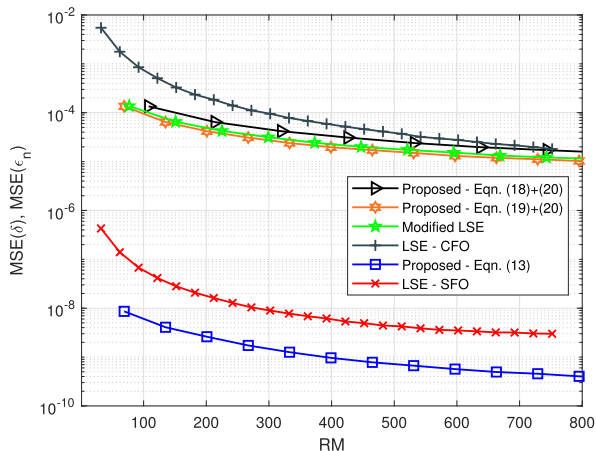


FIGURE 10. MSE of the SFO and of the CFO estimates vs. the number of RMs, with  $\epsilon_n = 0.01$ , and  $\delta = 2 \cdot 10^{-4}$  for CH1, at  $E_b/N_0 = 20$  [dB].

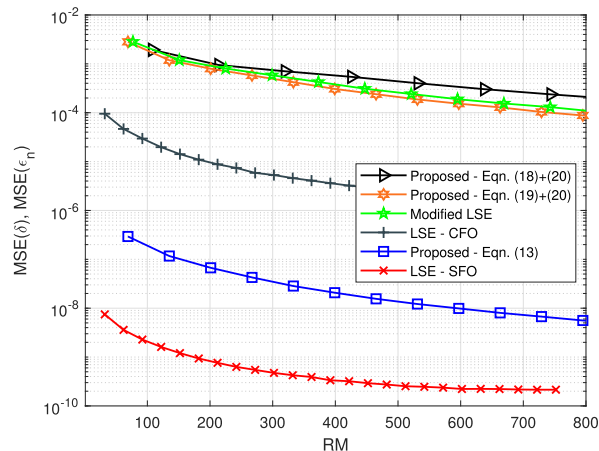


FIGURE 11. MSE of the SFO and of the CFO estimates vs. the number of RMs, with  $\epsilon_n = 0.01$ , and  $\delta = 2 \cdot 10^{-4}$  for CH2, at  $E_b/N_0 = 20$  [dB].

estimators depends on  $|\mathcal{N}_{\text{SFO}}|$ , and can vary from linear to quadratic dependence on  $|\mathcal{K}_p|$ . In the numerical performance evaluations we use 2 pilot subcarriers for the SFO and the CFO estimators in the proposed algorithms. In [21, Tab. 2] it was suggested that the number of iterations needed to achieve a sufficient accuracy for a real division is 2, therefore, we obtain that the complexity of proposed SFO estimator combined with the proposed CFO estimator  $\hat{\epsilon}_n^{(1)}$ , totals at 116 RMs, the proposed SFO estimator combined with the proposed CFO estimator  $\hat{\epsilon}_n^{(2)}$ , has a complexity of 77 RMs, and the proposed SFO estimator combined with the modified LSE algorithm has a complexity of 86 RMs. Note that in the proposed CFO estimators,  $\hat{\epsilon}_n^{(1)}$  and  $\hat{\epsilon}_n^{(2)}$ , the multiplication by the constant  $1/|\mathcal{K}_p| = 0.5$  in the computation of the average estimate does not incur computational complexity, since it can be implemented by shifting. Also note that as  $|\mathcal{N}_{\text{SFO}}| = 1$ , multiplication by  $1/|\mathcal{N}_{\text{SFO}}| = 1$  in the proposed SFO estimator,  $\hat{\delta}$ , does not incur computational complexity. The LSE operates with 6 pilot subcarriers resulting in a complexity of 92 RMs. Lastly, the LHHYW operates with  $K = 14$  subcarriers, which results in a complexity of 130 RMs for a single grid search point, while its approximated SFO estimator version requires 2906 RMs, see Appendix B. We observe that the computational complexities of the new algorithms are considerably lower than that of LHHYW algorithm, and are similar to that of the LSE algorithm. However, the new algorithms do not restrict the pilot subcarrier indexes and can work for any set of OFDM subcarrier indexes. Next, we examine the relationship between MSE performance and the computational complexity of the different schemes, by varying the number of pilots and evaluating the performance of the different estimators. To reduce clutter, we present here only the performance of the LSE and of the proposed algorithms with the SFO estimated via (13) and the CFO estimated via either (18) or (19) as well as via the modified LSE based on Eqn. (23). From Fig. 10 we observe that for CH1, the performance of the LSE as well as of the proposed algorithms

improve as the RM complexity increases, however, for both the SFO estimate and the CFO estimate, the performance of the proposed estimators are consistently better than those of the LSE estimator in the tested range. In fact, for SFO estimation, as RM complexity increases, the MSE of the LSE floors at a higher value than the MSE of the proposed scheme. For the CFO estimate, as RM complexity increases, the MSE performance of the LSE CFO estimate approaches that of the proposed schemes, yet, it remains higher than that of the proposed schemes in the tested range. We note that further increasing the RM complexity we obtain that the MSE of the LSE CFO estimator crosses that of Eqn. (18) at some higher RM complexity, but remains higher than the MSEs of the other CFO estimators. For CH2, it is observed from Fig. 11 that, while performance of both the proposed estimators and of the LSE estimator improve as the computational complexity increases, the LSE is superior to the proposed schemes for the entire range of RM complexity tested. We observe that when RM complexity increases, performance improves until it reaches a floor. For CH2, the proposed CFO estimator has a higher floor compared that the LSE estimator, likely because of ignoring the noise in the derivation of the cost function. We conclude that the proposed SFO and CFO estimators of Eqns. (13) and (19) are superior to the LSE for many scenarios, at any RM complexity, yet there are scenarios in which the situation is reversed. As the focus is naturally on low complexity, we maintain that there is a strong motivation for the proposed algorithm.

In terms of the required a-priori information by the new SFO and the CFO estimation algorithms, we conclude that partial a-priori information on the magnitudes of the channel frequency response at the transmitter can improve the performance of the SFO and the CFO estimators in terms of their MSEs, by facilitating selection of strong pilot subcarriers. On the other hand, the numerical performance evaluations show that the new estimators can achieve good performance also without any a-priori information on the channel

frequency response. Both the LSE algorithm and the new algorithms require a-priori information regarding the pre-defined pilots sets, while the LHHYW does not require any a-priori information as its SFO and CFO estimations are not based on pilots subcarriers, yet it requires a-priori information about the ISI duration, as the LHHYW algorithm needs to identify a shifted FFT window which contains ISI-free CP samples.

## VI. CONCLUSIONS

In this paper, we derived low complexity algorithms for the estimation of CFO and SFO based on known pilots in OFDM systems, assuming the channel remains constant over two consecutive OFDM symbols. The algorithm first estimates the SFO and then proceeds to estimate the CFO for which we propose two new estimators, as well as a modification to that of [9]. Numerical evaluations show that there are many scenarios in which the new estimators are superior to the current schemes, but there are also many scenarios in which the opposite is true. Further research is required in order to find ways to combine the two estimators to benefit from their advantages in all scenarios. In recent years, machine learning (MCL) has been considered for multiple problems in which the expert systems (ESs) have a high computational complexity. We note that application of MCL to estimation of physical parameters have been largely unexplored. Recently, several works have studied parameter estimation based on machine learning, such as [19], in which three classes of deep neural network (DNN)-based CFO estimation for IEEE 802.11ah, were proposed. The tests carried out in [19] showed that the expert system has outperformed the MCL-based estimator. In [22], a DNN was developed for estimating the pitch frequency for noisy speech or music signals. It was observed that the proposed DNN pitch estimator achieves performance similar to the expert systems. Some works did report superior performance over that of the ES, e.g., the frequency estimation works in [23], [24], however, complexity of the different schemes was not reported, and applicability to modulated signals was not discussed in [23]. We thus conclude that while there is no conclusive evidence to the usefulness of MCL for parameter estimation, it is definitely a research direction that we are considering in our current research, presently focusing on model-based approaches.

## APPENDIX A COMPUTATIONAL COMPLEXITY ANALYSIS FOR LSE METHOD

The LSE estimator first computes complex multiplications of pairs of symbols, see [9, Eqn. (2)],  $Y_{m,k} = R_{m,k}^* R_{m+1,k}$ , which requires  $4|\mathcal{K}_p|$  RMs and  $2|\mathcal{K}_p|$  RAs for  $|\mathcal{K}_p| \geq 2$ . Then, the summation term  $\Lambda_1$  in [9, Eqn. (10)],  $\Lambda_1 = \sum_{k \in \mathcal{S}_1} \arg\{Y_{m,k}\} + \sum_{k \in \mathcal{S}_2} \arg\{Y_{m,k}\}$ , where  $\mathcal{S}_1$  and  $\mathcal{S}_2$  are a partition of the set of pilot subcarrier indexes, is evaluated using the inverse trigonometric function  $\tan^{-1}(\cdot)$ , which requires a real division for computing the argument, after which the arguments are summed. Thus, computation of  $\Lambda_1$

entails an overall cost of  $|\mathcal{K}_p|(2i + 6)$  RMs and  $|\mathcal{K}_p|(i + 3) - 1$  RAs. Next, the CFO estimate in [9, Eqn. (14)],  $\hat{\epsilon}_n = \Lambda_1 / (2\pi\rho N_p)$  is evaluated (where  $\rho = N_{\text{sym}}/N_{\text{sc}}$ ) with a single real multiplication by a constant,  $1/(2\pi\rho N_p)$ , which requires 1 RM, where it is assumed that  $1/(2\pi\rho N_p)$  has been computed previously. Subsequently, the summation term,  $\Lambda_2$ , in [9, Eqn. (12)],  $\Lambda_2 = \sum_{k \in \mathcal{S}_1} k \cdot \arg\{Y_{m,k}\} + \sum_{k \in \mathcal{S}_2} k \cdot \arg\{Y_{m,k}\}$  is evaluated at an overall cost of  $|\mathcal{K}_p|$  RMs and  $|\mathcal{K}_p| - 1$  RAs. Note that the terms  $\arg\{Y_{m,k}\}$  have already been evaluated for computing  $\Lambda_1$ . Then, the SFO estimate in [9, Eqn. (15)],  $\hat{\delta} = \Lambda_2 / (2\pi\rho M_p)$ , is evaluated with a single real multiplication by the constant  $1/(2\pi\rho M_p)$ ,  $M_p \triangleq \sum_{k \in \mathcal{S}_1} k^2 + \sum_{k \in \mathcal{S}_2} k^2$ , which requires 1 RM, again assuming that  $1/(2\pi\rho M_p)$  has been previously computed. Thus, the overall complexity is  $|\mathcal{K}_p|(2i + 11) + 2$  RMs and  $|\mathcal{K}_p|(i + 6) - 2$  RAs.

## APPENDIX B COMPUTATIONAL COMPLEXITY ANALYSIS FOR THE LHHYW METHOD

### A. A SINGLE DIMENSION GRID SEARCH FOR THE LHHYW SFO ESTIMATOR

The LHHYW estimator first computes the term  $\Theta(\tilde{\delta})$  in [10, Eqn. (31)],  $\Theta(\tilde{\delta}) = \sum_{k=-K/2, k \neq 0}^{K/2} R_{m,k,L}^* R_{m,k,L} e^{-j\frac{2\pi}{N_{\text{sc}}} kL(1+\tilde{\delta})}$ ,  $K = |\mathcal{K}_p|$ , which requires two complex multiplications for each summand, as well as a complex summation over  $K - 1$  subcarriers. Therefore, this step requires  $8K$  RMs and  $6K - 2$  RAs, assuming the complex exponents  $e^{-j2\pi kL(1+\tilde{\delta})/N_{\text{sc}}}$  have already been computed (note that  $\tilde{\delta}$  is a grid search point). Then, implementing of the  $\arg\max_{\tilde{\delta}} |\Theta(\tilde{\delta})|^2$ , requires a complex norm operation at each grid search point, which uses 2 RMs and 1 RA. Next, the CFO estimate in [10, Eqn. (33)],  $\hat{\epsilon}_n = N_{\text{sc}} \cdot \arg\{\Theta(\hat{\delta})\} / (2\pi L(1+\hat{\delta}))$  is evaluated using a real division of the imaginary part by the real part ( $2i + 1$  RMs,  $i$  RAs) followed by the inverse trigonometric function  $\tan^{-1}(\cdot)$  ( $5$  RMs,  $2$  RAs). Then, a real addition ( $0$  RMs,  $1$  RA) and a real division ( $2i + 1$  RMs,  $i$  RAs) involving the SFO estimate are applied for obtaining  $\arg\{\Theta(\hat{\delta})\} / (1 + \hat{\delta})$ , and lastly, a real multiplication by a constant  $N_{\text{sc}}/2\pi L$  is applied ( $1$  RM,  $0$  RAs), assuming the constant  $N_{\text{sc}}/2\pi L$  has been a-priori evaluated. The total complexity of the CFO estimate is thus  $4i + 8$  RMs and  $2i + 3$  RAs. Thus, the overall complexity is  $8K + 4i + 10$  RMs and  $6K + 2i + 2$  RAs. Note that the computational complexity for LHHYW was evaluated for a single grid search point.

### B. APPROXIMATED LHHYW SFO ESTIMATOR

We present a brief summary of the computational complexity for the approximated LHHYW SFO estimator: The LHHYW first computes the term in [10, Eqn. (37)],  $f(\delta_0) = \sum_{p \neq q} (p - q) R_{m,p,L}^* R_{m,p,L} R_{m,q,L} R_{m,q,L}^* e^{j\frac{2\pi}{N_{\text{sc}}} L(p-q)(1+\delta_0)}$ , which requires  $K(5K - 1)$  RMs and  $K(5K - 3)$  RAs ( $\delta_0$  is a known initial value). Then, the term in [10, Eqn. (39)],  $w = \delta_0 - f(\delta_0)/f'(\delta_0)$ , requires  $K(K - 1) + 2i + 1$  RMs and  $2K(K - 1) + i + 1$  RAs. Lastly, the SFO estimate is obtained via: [10, Eqn. (38)],  $\hat{\delta} = w - f(w)f'(w) / \left( (f'(w))^2 - f(w)f''(w)/2 \right)$ ,

which requires  $19K(K-1)/2 + 2i + 4$  RMs and  $9K(K-1) + i + 3$  RAs. Thus, the overall complexity combined with the CFO estimator in [10, Eqn. (33)] is  $K(31K-23)/2 + 8i + 13$  RMs and  $K(15K-13) + 4i + 7$  RAs.

## REFERENCES

- [1] P. Guan, D. Wu, T. Tian, J. Zhou, X. Zhang, L. Gu, A. Benjebbour, M. Iwabuchi, and Y. Kishiyama, "5G field trials: OFDM-based waveforms and mixed numerologies," *IEEE J. Sel. Areas Commun.*, vol. 35, no. 6, pp. 1234–1243, Jun. 2017.
- [2] A. Ali, R. Vesilo, and M. Di Renzo, "Stochastic geometry analysis of multi-user asynchronous OFDM wireless networks," *IEEE Wireless Commun. Lett.*, vol. 8, no. 3, pp. 845–848, Jun. 2019.
- [3] K. Shi, E. Serpedin, and P. Ciblat, "Decision-directed fine synchronization in OFDM systems," *IEEE Trans. Commun.*, vol. 53, no. 3, pp. 408–412, Mar. 2005.
- [4] M. Morelli and M. Moretti, "Fine carrier and sampling frequency synchronization in OFDM systems," *IEEE Trans. Wireless Commun.*, vol. 9, no. 4, pp. 1514–1524, Apr. 2010.
- [5] Y. Murin and R. Dabora, "Low complexity estimation of carrier and sampling frequency offsets in burst-mode OFDM systems," *Wireless Commun. Mobile Comput.*, vol. 16, no. 9, pp. 1018–1034, Jun. 2016.
- [6] H.-G. Jeon, K.-S. Kim, and E. Serpedin, "An efficient blind deterministic frequency offset estimator for OFDM systems," *IEEE Trans. Commun.*, vol. 59, no. 4, pp. 1133–1141, Apr. 2011.
- [7] S. Lmai, A. Bourre, C. Laot, and S. Houcke, "An efficient blind estimation of carrier frequency offset in OFDM systems," *IEEE Trans. Veh. Technol.*, vol. 63, no. 4, pp. 1945–1950, May 2014.
- [8] C. Chen, Y. Chen, N. Ding, Y. Wang, J.-C. Lin, X. Zeng, and D. D. Huang, "Accurate sampling timing acquisition for baseband OFDM power-line communication in non-Gaussian noise," *IEEE Trans. Commun.*, vol. 61, no. 4, pp. 1608–1620, Apr. 2013.
- [9] Y.-A. Jung, J.-Y. Kim, and Y.-H. You, "Complexity efficient least squares estimation of frequency offsets for DVB-C2 OFDM systems," *IEEE Access*, vol. 6, pp. 35165–35170, Jun. 2018.
- [10] X. Li, J. Hu, W. Heng, F. Yu, and G. Wang, "Blind carrier and sampling frequency offsets estimation in OFDM system," in *Proc. IEEE Wireless Commun. Netw. Conf. (WCNC)*, San Francisco, CA, USA, Mar. 2017, doi: 10.1109/WCNC.2017.7925909.
- [11] N. Shlezinger and R. Dabora, "Frequency-shift filtering for OFDM signal recovery in narrowband power line communications," *IEEE Trans. Commun.*, vol. 62, no. 4, pp. 1283–1295, Apr. 2014.
- [12] K. Manolakis, C. Oberli, V. Jungnickel, and F. Rosas, "Analysis of synchronization impairments for cooperative base stations using OFDM," *Int. J. Antennas Propag.*, vol. 2015, Apr. 2015, Art. no. 125653, doi: 10.1155/2015/125653.
- [13] Y.-A. Jung, M.-Y. Kim, H.-K. Song, and Y.-H. You, "Blind weighted least-squares frequency offset estimation method for LTE machine-type communications," *IEEE Internet Things J.*, vol. 6, no. 6, pp. 9806–9815, Dec. 2019.
- [14] Y.-A. Jung and Y.-H. You, "Efficient weighted least-squares frequency synchronization scheme for digital terrestrial broadcasting system," *IEEE Trans. Broadcast.*, vol. 66, no. 2, pp. 359–364, Jun. 2020.
- [15] M. Speth, S. Fechtel, G. Fock, and H. Meyr, "Optimum receiver design for OFDM-based broadband transmission. II. A case study," *IEEE Trans. Commun.*, vol. 49, no. 4, pp. 571–578, Apr. 2001.
- [16] M. J. Flynn, "On division by functional iteration," *IEEE Trans. Comput.*, vol. C-19, no. 8, pp. 702–706, Aug. 1970.
- [17] R. L. Smith, "Algorithm 116: Complex division," *Commun. ACM*, vol. 5, no. 8, p. 435, Aug. 1962.
- [18] E. Khorov, A. Kiryanov, A. Lyakhov, and G. Bianchi, "A tutorial on IEEE 802.11ax high efficiency WLANs," *IEEE Commun. Surveys Tuts.*, vol. 21, no. 1, pp. 197–216, 1st Quart., 2019.
- [19] V. Ninkovic, D. Vukobratovic, A. Valka, and D. Domic, "Deep learning based packet detection and carrier frequency offset estimation in IEEE 802.11ah," 2020, *arXiv:2004.11716*. [Online]. Available: <http://arxiv.org/abs/2004.11716>
- [20] A. A. Karatsuba, "The complexity of computations," *Proc. Steklov Inst. Math.*, vol. 211, pp. 169–183, Jan. 1995.
- [21] N. M. Nenadic and S. B. Mladenovic, "Fast division on fixed-point DSP processors using Newton-Raphson method," in *Proc. IEEE Int. Conf. 'Comput. Tool' EUROCON*, Belgrade, Serbia, Nov. 2005, pp. 705–708.
- [22] P. Verma and R. W. Schafer, "Frequency estimation from waveforms using multi-layered neural networks," in *Proc. Annu. Conf. Int. Speech Commu. Assoc. (INTERSPEECH)*, San Francisco, CA, USA, Sep. 2016, pp. 2165–2169.
- [23] G. Izacard, S. Mohan, and C. Fernandez-Granda, "Data-driven estimation of sinusoid frequencies," in *Proc. Conf. Neural Inf. Process. Syst. (NeurIPS)*, Vancouver, BC, Canada, Dec. 2019, pp. 2165–2169.
- [24] J. Liu, K. Mei, X. Zhang, D. McLernon, D. Ma, J. Wei, and S. A. R. Zaidi, "Fine timing and frequency synchronization for MIMO-OFDM: An extreme learning approach," submitted to the *IEEE J. Sel. Areas Commun. Ser. Mach. Learn. Commun. Netw.* [Online]. Available: <https://arxiv.org/abs/2007.09248>



**ARIK ROTEM** (Student Member, IEEE) received the B.Sc. degree in electrical and computer engineering from Ben-Gurion University, Israel, in 2019, where he is currently pursuing the M.Sc. degree in electrical and computer engineering. His research interests include signal processing for communication, cyclostationary signal processing, and machine learning application in communication.



**RON DABORA** (Senior Member, IEEE) received the B.Sc. and M.Sc. degrees in electrical engineering from Tel-Aviv University, in 1994 and 2000, respectively, and the Ph.D. degree from Cornell University, in 2007. From 1994 to 2000, he was with the Ministry of Defense of Israel. From 2000 to 2003, he was with the Algorithms Group, Millimetrix Broadband Networks Ltd., Israel, and from 2007 to 2009, he was a Postdoctoral Researcher with the Department of Electrical Engineering, Stanford University. Since 2009, he has been with the Department of Electrical and Computer Engineering, Ben-Gurion University, Israel, where he is currently an Associate Professor. His research interests include network information theory, wireless communications, and power line communications. He served as a TPC member of a number of international conferences, including WCNC, PIMRC, and ICC, and he was the Keynote Speaker at ISPLC 2020. From 2012 to 2014, he was an Associate Editor of the IEEE SIGNAL PROCESSING LETTERS. He was a Senior Area Editor of the IEEE SIGNAL PROCESSING LETTERS, from 2014 to 2019.